END

FILMED

DTIC

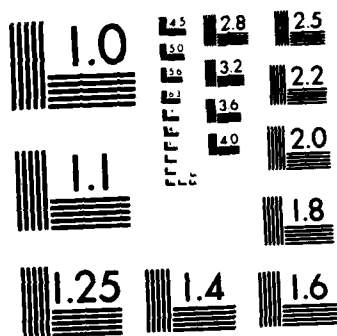MICROCOPY RESOLUTION TEST CHART

NATIONAL BUREAU OF STANDARDS-1963-A

REPORT NO. NADC-80130-60

AD-A145 372

EXPERIMENTAL INVESTIGATION OF THE INTERACTION OF MOISTURE, LOW TEMPERATURE, AND LOW LEVEL IMPACT ON GRAPHITE/EPOXY COMPOSITES-II
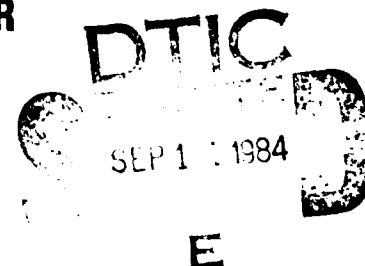
PREPARED BY

K. N. LAURAITIS
P.E. SANDORFF

LOCKHEED-CALIFORNIA COMPANY
BURBANK, CALIFORNIA

FINAL REPORT
OCTOBER 1982

DTIC FILE COPY

PREPARED FOR
NAVAL AIR DEVELOPMENT CENTER
WARMINSTER, PENNSYLVANIA

CONTRACT NO. N62269-80-C-0709

DTIC

SEP 1 1984

E

84 09 13 062

NOTICES

REPORT NUMBERING SYSTEM — The numbering of technical project reports issued by the Naval Air Development Center is arranged for specific identification purposes. Each number consists of the Center acronym, the calendar year in which the number was assigned, the sequence number of the report within the specific calendar year, and the official 2-digit correspondence code of the Command Office or the Functional Directorate responsible for the report. For example: Report No. NADC-78015-20 indicates the fifteenth Center report for the year 1978, and prepared by the Systems Directorate. The numerical codes are as follows:

CODE	OFFICE OR DIRECTORATE
00	Commander, Naval Air Development Center
01	Technical Director, Naval Air Development Center
02	Comptroller
10	Directorate Command Projects
20	Systems Directorate
30	Sensors & Avionics Technology Directorate
40	Communication & Navigation Technology Directorate
50	Software Computer Directorate
60	Aircraft & Crew Systems Technology Directorate
70	Planning Assessment Resources
80	Engineering Support Group

PRODUCT ENDORSEMENT — The discussion or instructions concerning commercial products herein do not constitute an endorsement by the Government nor do they convey or imply the license or right to use such products.

SECURITY CLASSIFICATION OF THIS PAGE (When Data Entered)

REPORT DOCUMENTATION PAGE		READ INSTRUCTIONS BEFORE COMPLETING FORM
1. REPORT NUMBER NADC-80130-60	2. GOVT ACCESSION NO. AD-A145372	3. RECIPIENT'S CATALOG NUMBER
4. TITLE (and Subtitle) EXPERIMENTAL INVESTIGATION OF THE INTERACTION OF MOISTURE, LOW TEMPERATURE, AND LOW LEVEL IMPACT ON GRAPHITE/EPOXY COMPOSITES II		5. TYPE OF REPORT & PERIOD COVERED FINAL REPORT
		6. PERFORMING ORG. REPORT NUMBER
7. AUTHOR(s) K. N. LAURAITIS P. E. SANDORFF		8. CONTRACT OR GRANT NUMBER(s) N62269-80-C-0709
9. PERFORMING ORGANIZATION NAME AND ADDRESS Lockheed-California Company Burbank, CA 91520		10. PROGRAM ELEMENT, PROJECT, TASK AREA & WORK UNIT NUMBERS
11. CONTROLLING OFFICE NAME AND ADDRESS Naval Air Systems Command Department of the Navy Washington, DC 20361		12. REPORT DATE OCTOBER 1982
		13. NUMBER OF PAGES 62
14. MONITORING AGENCY NAME & ADDRESS(if different from Controlling Office) Naval Air Development Center Department of the Navy Warminster, PA 18974		15. SECURITY CLASS. (of this report) UNCLASSIFIED
		15a. DECLASSIFICATION/DOWNGRADING SCHEDULE

16. DISTRIBUTION STATEMENT (of this Report)

APPROVED FOR PUBLIC RELEASE: DISTRIBUTION UNLIMITED

17. DISTRIBUTION STATEMENT (of the abstract entered in Block 20, if different from Report)

18. SUPPLEMENTARY NOTES

19. KEY WORDS (Continue on reverse side if necessary and identify by block number)

20. ABSTRACT (Continue on reverse side if necessary and identify by block number)

DD FORM 1473 EDITION OF 1 NOV 65 IS OBSOLETE
1 JAN 73
S/N 0102-LF-014-6601

SECURITY CLASSIFICATION OF THIS PAGE (When Data Entered)

This Page Intentionally Left Blank

FOREWORD

Accession For	
NTIS GRA&I	X
DTIC TAB	☐
Unannounced	☐
Justification	
By	
Distribution/	
Availability Codes	
Dist	Avail and/or Special
A-1	

DTIC COPY INSPECTED

This Page Intentionally Left Blank

TABLE OF CONTENTS

This Page Intentionally Left Blank

LIST OF FIGURES

LIST OF FIGURES - CONTINUED

LIST OF FIGURES - CONTINUED

This Page Intentionally Left Blank

LIST OF TABLES

SECTION 1
INTRODUCTION

1.1 PROBLEM DEFINITION

Effect of low speed impact damage on composite materials is a new and po-
tentially significant design condition for high performance systems. In
metallic structure, damage due to tool drop, small rock impact and hail
(while on the ground) did not constitute a damage of major concern. How-
ever, composites generally exhibit little inelastic ductility, are sensitive
to secondary stresses, and are susceptible to splitting and delamination
with cracks often propagating in the fiber direction through debonding.
Upon failure, energy absorption is low. Due to these fracture character-
istics and the low strain to failure, composite materials generally exhibit
lower impact resistance than the metals typically used for aircraft con-
struction.

Environmental exposure may aggravate the deleterious effects of impact
damage. It is well known that the mechanical properties of a polymeric
matrix are susceptible to environmental degradation. Matrix cracking re-
sulting from impact loading or thermal cycling may provide pathways for
moisture which can enter by laminar flow much more rapidly than by diffusion
upon subsequent exposure to a high humidity environment at elevated
temperatures . Detrimental effects may also be expected because the
internal tensile stress in the matrix increases with decreasing temperature,
promoting crazing and the formation of microvoids. Futhermore, the cubical
coefficient of expansion of epoxy polymers is approximately $1.5 \times 10^{-6}\ °C^{-1}$
and that of ice approximately $112 \times 10^{-6}\ °C^{-1}$ down to $-54°C$ ($-65°F$); thus,
ice formation in the matrix cracks may promote crazing and crack growth on
cooldown to this temperature. The possible degradation of compressive

strength due to temperature and moisture has thus been one of the major concerns in the application of advanced composite systems to aircraft structure. Interactions between impact damage and environmental factors and their combined effect upon compression buckling strength have been examined under a previous Navy contract, N62269-79-C-0276, of the same title, wherein the damage was limited to near visual surface damage produced by low speed, hard object impact such as dropped tools. This type of damage alone produced a reduction in the column compressive strength of twelve to fifteen percent. However, no further reduction in residual column strength was found to result from environmental exposure in combination with impact. This may have been due to a coincidence of test conditions which made the residual strength test insensitive to changes in the extent of the delaminated regions. The relatively thin 16-ply coupon required support under compressive loading through the damage region. Support outside of the damage area resulted in elastic Euler-like buckling which showed little re-duction in strength due to damage. For the configuration evaluated, buckling generally occurred below 0.006 in./in. in undamaged coupons. When buckling occurs at such low strains, damage does not appear to as severely reduce the strength as is known to occur at strains above 0.007 in./in. Thus the constraint conditions become an integral part of the test and the results must be evaluated for a particular structural system.

The intent of this investigation was to extend the previous effort to a more detailed examination of whether the interaction of impact damage and environmental factors can have a deleterious effect on graphite/epoxy laminates.

1.2 OBJECTIVE

The objective of this program was to provide an experimental evaluation of the possible interaction effects of environmental factors (specifically moisture and low temperature) with low velocity impact damage and thus to ascertain whether damage is likely to extend due to expansion of water

present in cracks as it freezes, and to determine whether low velocity impact damage will grow during freeze-thaw cycling.

1.3 PROGRAM SUMMARY

The type of damage investigated in this program included; a) that which is produced by low speed impact of a blunt object, such as an accidentally dropped hand tool; b) severe delamination produced by residual strength testing of an impact damaged specimen; and c) delamination produced by placing release film between two plies during fabrication. Specimens containing (a) and (b) type of damage (as noted above) were used in the first phase to experimentally determine:

o Amount of damage growth produced by the freeze-thaw cycle in representative impact damaged specimens.

o Amount of water picked up in the liquid state by the ruptured and delaminated regions of typical impact-damaged specimens.

o Whether water migrates into and out of damaged regions during freeze-thaw cycling.

Specimens containing (c) type damage were used in the second phase to experimentally determine the amount of crack opening displacement necessary (for a given crack length and initial displacement) to produce crack extension. These results were compared to the amount of displacement that might be expected due to the freezing of moisture.

This Page Intentionally Left Blank

SECTION 2
ENVIRONMENTAL EXPOSURE TESTS

This study utilized specimens from the previous contract effort, N62269-79-C-276, documented in Reference 1. Four impact-damaged specimens were selected from the preliminary test series of Reference 1, Table 4-1. These contained barely visible back surface damage with internal delaminations of approximately 1 1/8 - 1 1/2 inches in diameter. To evaluate the effect of severe damage, four specimens, which had been subjected to low velocity impact and subsequently tested in compression/buckling for residual strength, were selected from Group C-2, Table 5-1 (Reference 1). Delaminations for these specimens were on multiple layers and extended the entire width of the 3" wide coupons. Specimens were prepared by removing end tabs and drying at 150°F in vacuo for two weeks. Two undamaged traveller specimens of the same dimensions (9" x 3") were cut from trim stock of panel 1X01674 (Reference 1, page 2-2). After drying, all ten specimens were C-scanned, then immersed in water at 160°F for 18 days. However, there was an approximately one month delay between the drying and subsequent water immersion due to difficulties encountered with the Holscan ultrasonic unit. After all but two of the initial scans were completed, the transducer ceased to function. Efforts expended to repair this transducer were not successful nor were attempts to locate a replacement. Consequently, conventional through-transmission ultrasonic C-scanning was used for this study. To assess the effect of the delay on moisture pick-up, additional damaged and undamaged control coupons were cut from panel 1X01618. These were dried and immediately immersed in 160°F water for the same time period. The moisture absorption data are displayed in graphical form in Figures 2.1 and 2.2. Moisture absorption for specimens containing barely visible back surface damage was nearly identical to that of the undamaged control coupons indicating that additional moisture is not absorbed by the damaged region for this damage condition. However, as expected, considerably greater weight gain was recorded for the severely
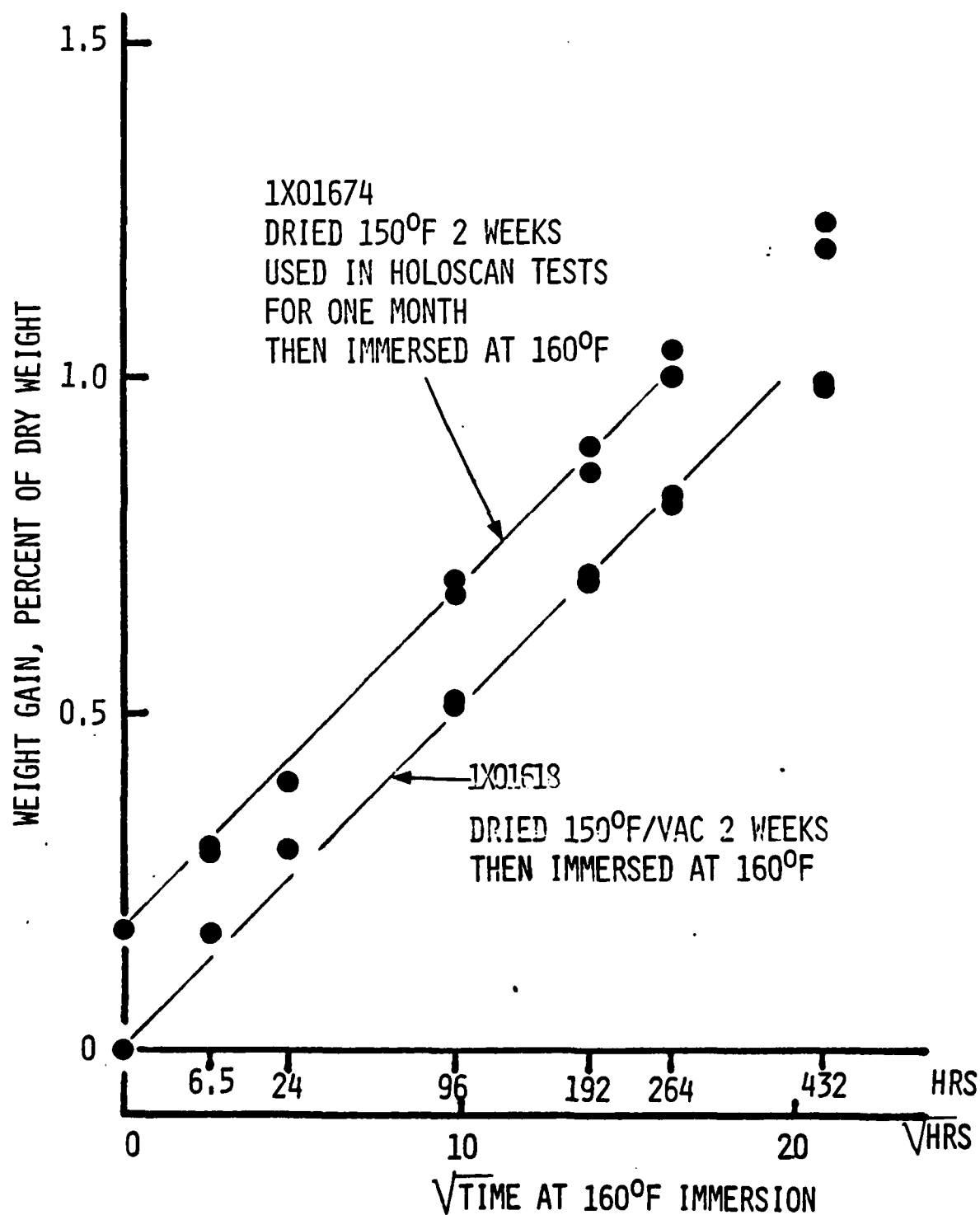
Figure 2.1: Moisture Absorption for Control (Undamaged) Coupons
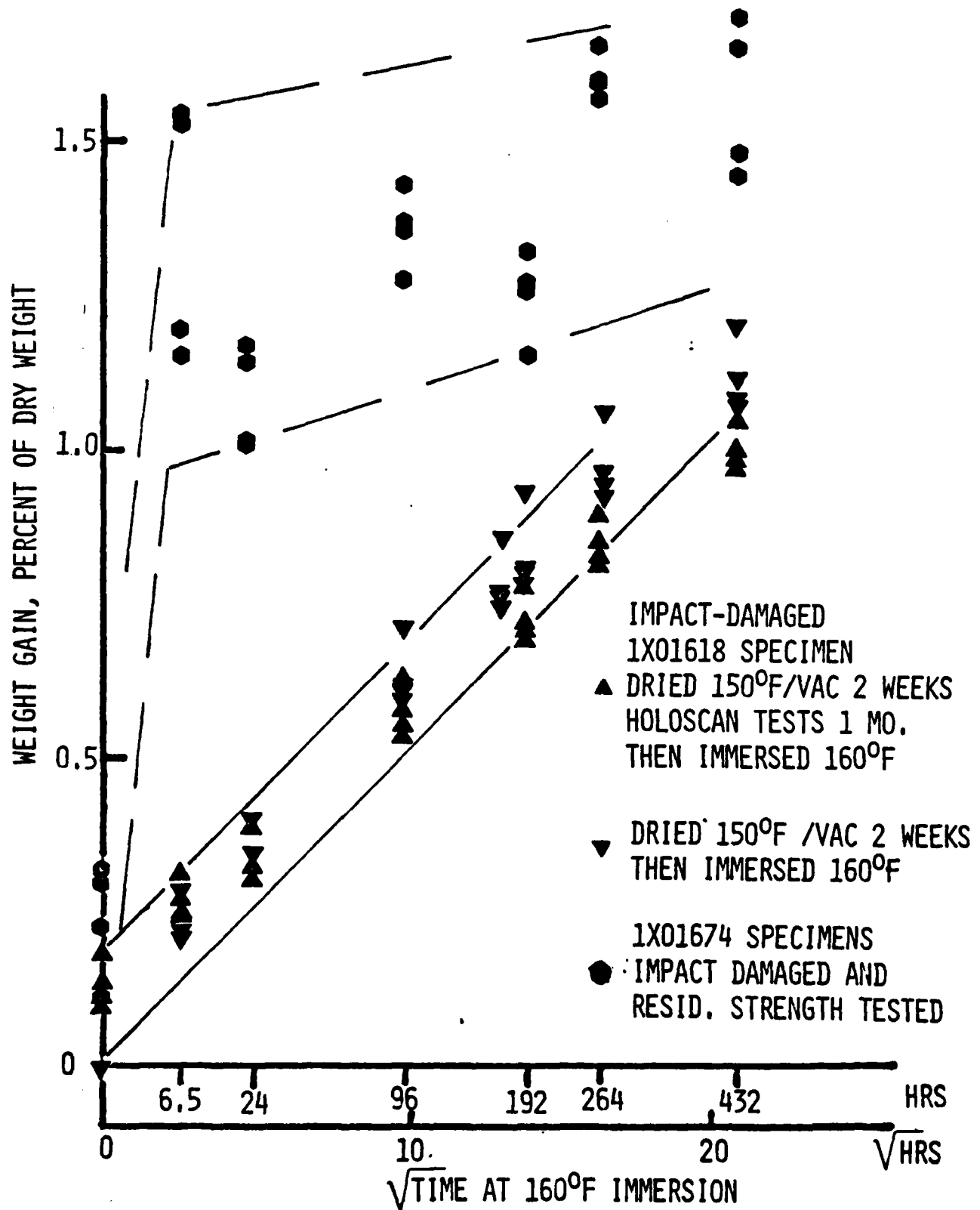
Figure 2.2: Moisture Absorption for Damaged Coupons

1X01674-1   1X01674-2

1X01674-10   1X01674-12

1X01618-3   1X01618-5   1X01618-8

1X01618-16   ½ in. NDI Standard   ¼ in. NDI Standard
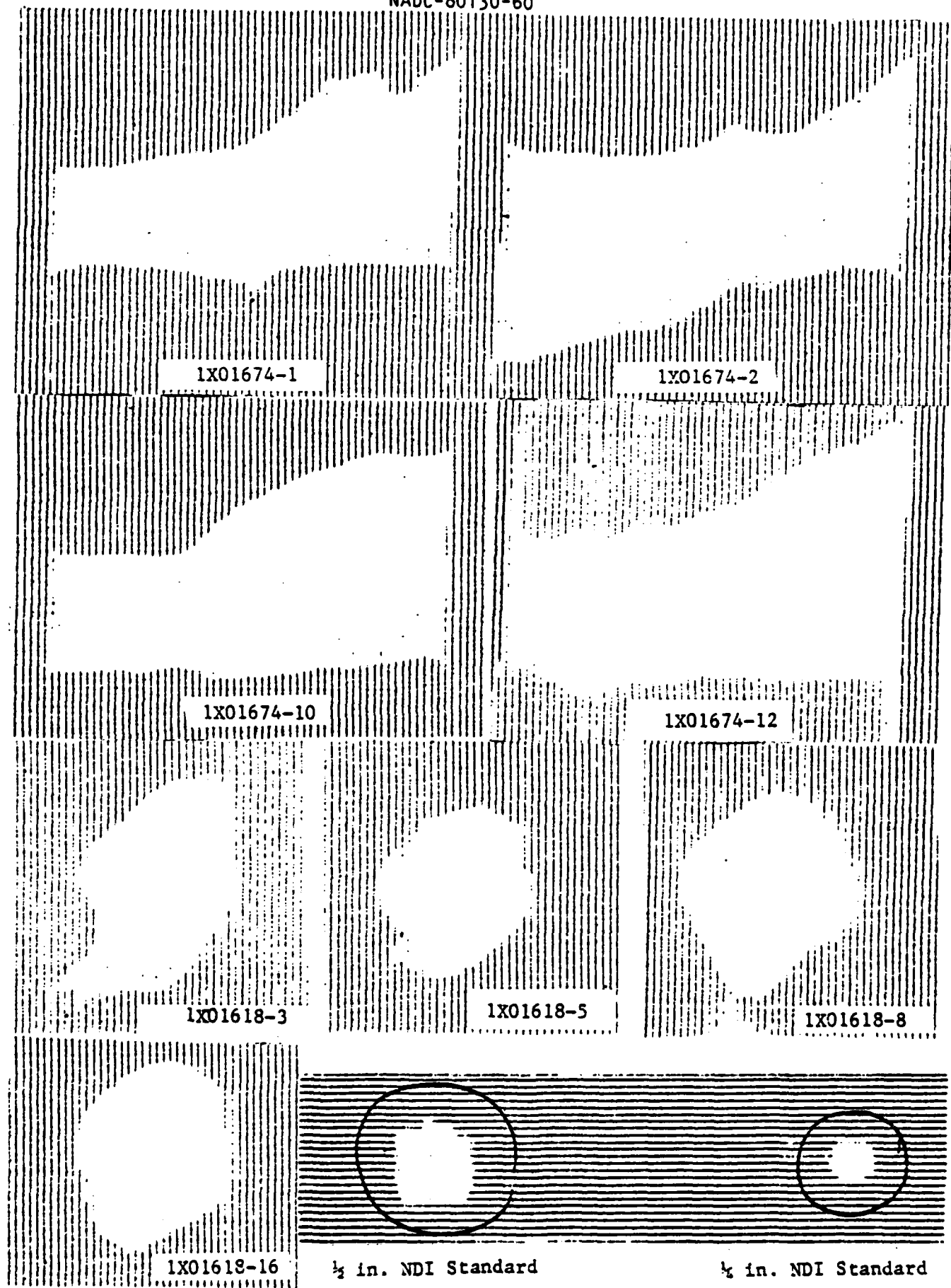
Figure 2.3:   C-Scans of Initial Damages In
Specimens to be Freeze-Thaw Cycled

1X01674-1   1X01674-2

1X01674-10   1X01674-12

1X01618-3   1X01618-5   1X01618-31   1X01618-16

½ in. NDI Standard   ¼ in. NDI Standard
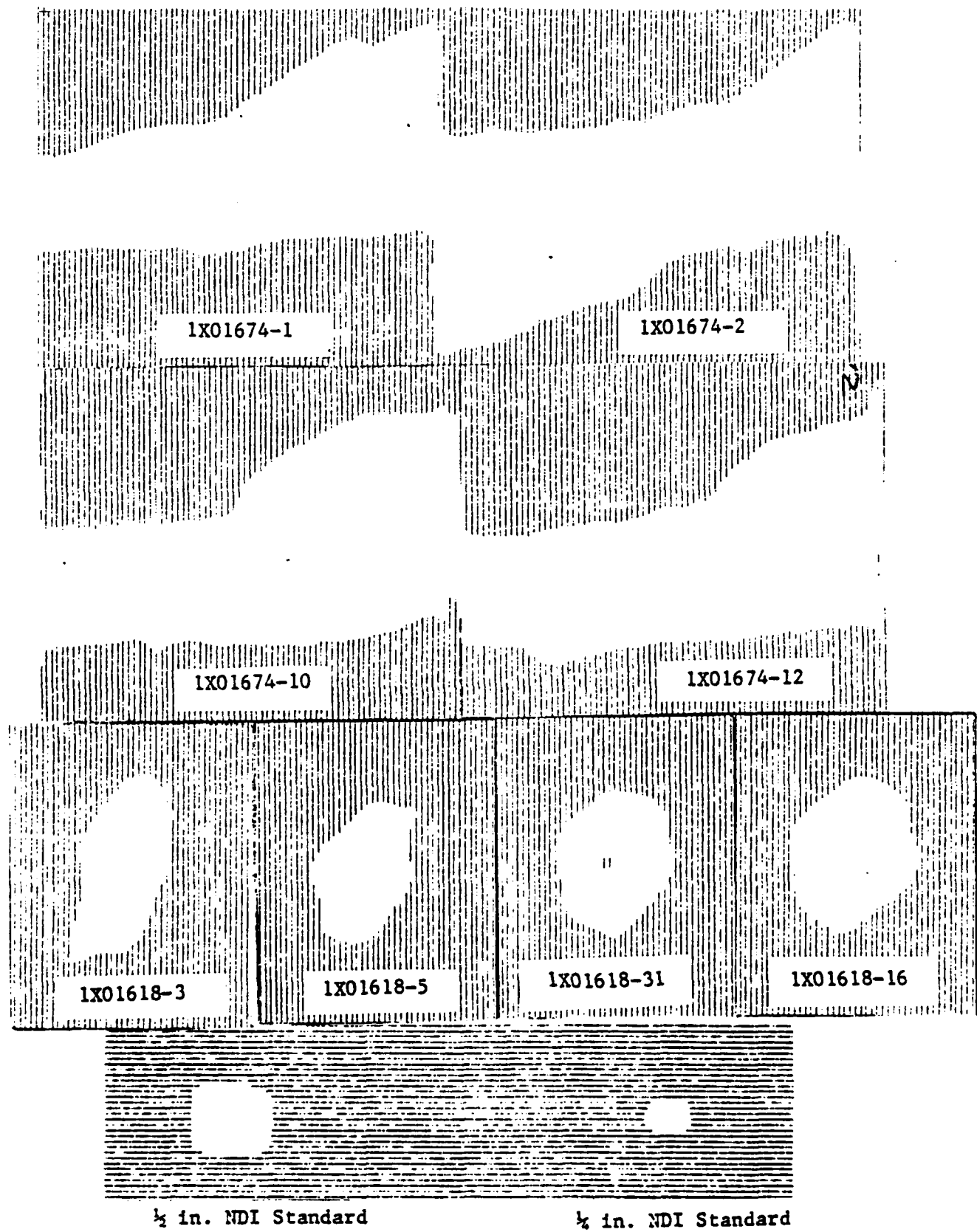
Figure 2.4:   C-Scans After One Hour Exposure
at $-65°$F

9

1X01674-1   1X01674-2

1X01674-10   1X01674-12

1X01618-3   1X01618-5   1X01618-8   1X01618-16

½ in. NDI Standard   ¼ in. NDI Standard
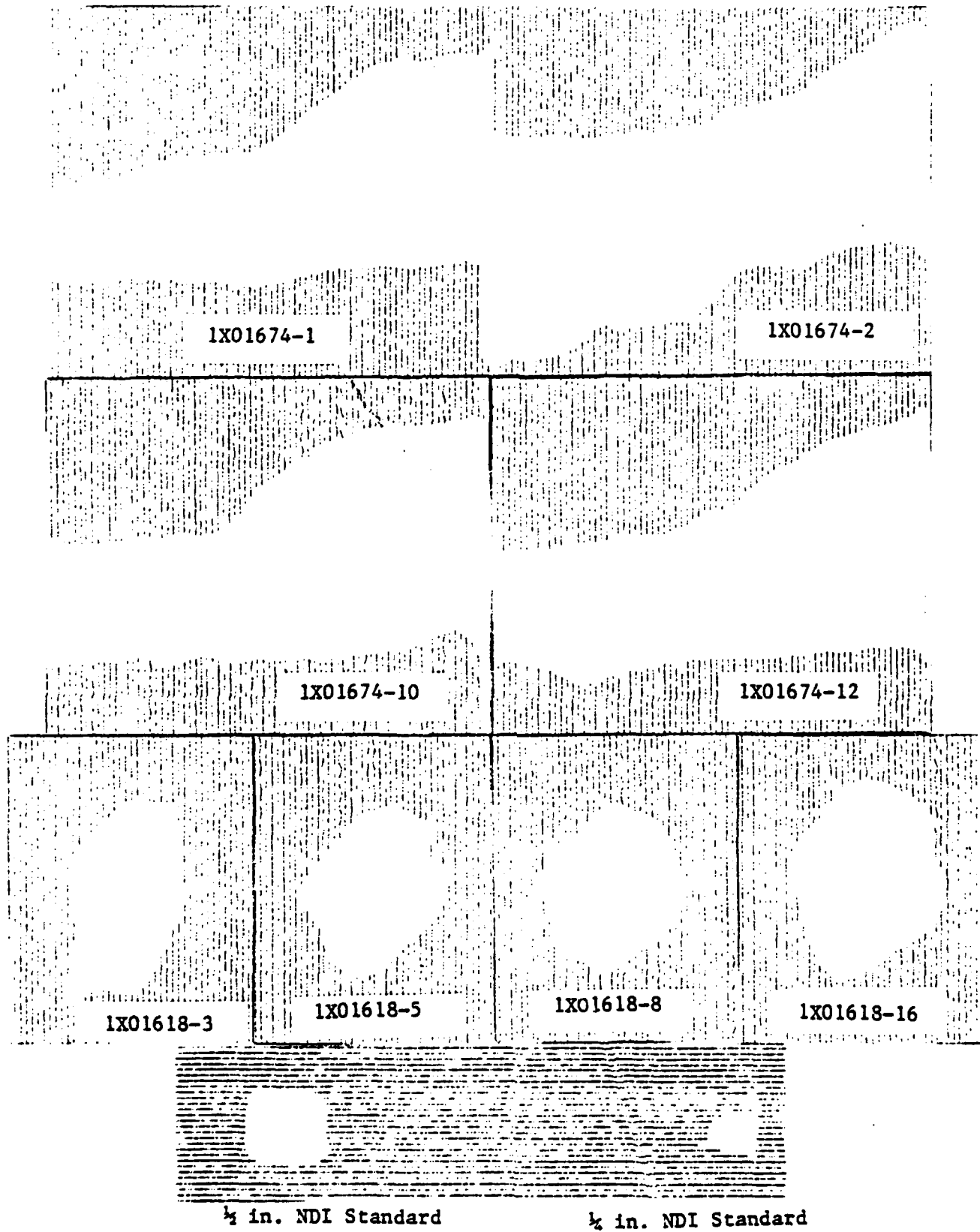
Figure 2.5:   C-Scans After Ten One Hour Cycles
of Alternating 160°F Immersion
with -65°F Exposure
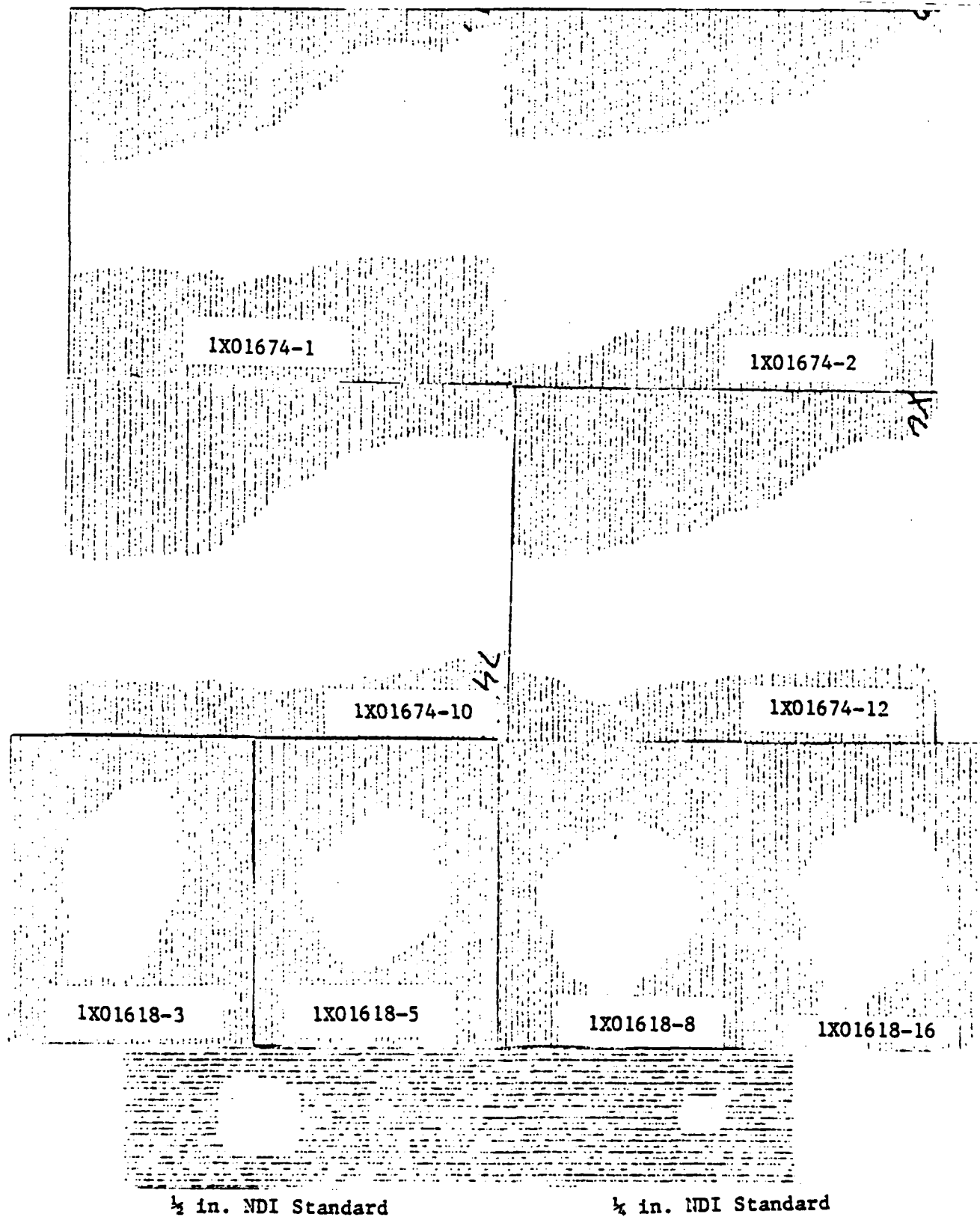
½ in. NDI Standard   ¼ in. NDI Standard

Figure 2.6:   C-Scans After Twenty One Hour
Cycles of Alternating 160°F
Immersion with -65°F Exposure

11

damaged residual strength tested specimens. The large data dispersion is due to the fact that water would pour from the specimens when they were removed for weighing making it difficult to obtain a stable weight reading.

After conditioning, specimens were then subjected to a one hour exposure at -65° and C-scanned again. The initial C-scans and scans after the -65°F exposure are presented in Figures 2.3 and 2.4, respectively. The C-scan damage size appears to be reduced after the conditioning and -65°F exposure. Although the C-scan technique used is not as accurate as the Holscan, it was not expected to show as large a change due to set-up. Such a loss in C-scan indications after moisture conditioning has been observed by others[2] and may be due to moisture altered transmission characteristics. Swelling of the laminate has also been observed to effect closure of some cracks[3]. However, it was ascertained that the initial scans were made on different equipment from all subsequent scans, since during this time the Lockheed Q.A. department had received new equipment and phased-out the old. The NDI standards do differ in size and it appears that the variation is probably due to differences in set-ups.

Little effect would be expected after the single hour exposure at -65°F and thus these scans can be used as a baseline for determining further growth. To confirm this postulation, two specimens were sent for scanning to Sigma Research which has equipment comparable to the Holscan. Comparison of their scans with the initial Holscans, which were made prior to equipment failure, indicate no growth of the damage region.

After the single cycle exposure at -65°F, specimens were subjected to ten cycles of immersion at 160°F for one hour followed by exposure to -65°F for one hour. These were then returned to room temperature, weighed, C-scanned, and another ten hygrothermal cycles were applied. Specimens were once again weighed and C-scanned. Ultrasonic C-scans for the first and second set of ten cycle exposures are displayed in Figures 2.5 and 2.6. There is some variation in the damage size which appears to be due to the lack of exact

12

reproducibility of the equipment for each set-up. Examination of these damage sizes seems to indicate that no growth is occurring. However if any growth were occurring after only a small number of cycles it should be of detectable dimensions after the application of a much larger number of cycles. Thus an additional 79 cycles of $160^{\circ}F$ immersion alternating with $-65^{\circ}F$ exposure were applied for a total of 99 cycles. C-Scans after the 99 cycle exposure are presented in Figure 2.7. No growth of the damage areas is evident. These results are greatly reassuring and in agreement with those reported in a recently completed Air Force sponsored program[4]. In this study, containing a badly delaminated hole, with initial damage dimensions of approximately 0.6 inch x 0.8 inch, were subjected to fully reversed fatigue cycling with maximum stress on the order of 50% of the static strength. Even under such severe conditions thousands of cycles were required before measurable growth was recorded. Because this material has a relatively high tensile strength as compared to other materials, such as concrete or rock, which are known to fail due to ice formation, extremely high stresses would have to be developed as a result of expanding ice to promote growth of the damage. Damage produced by impact usually has an associated loss in stiffness of the outer layers making it more difficult to develop the high stresses.

Also, impact damage is usually not confined to a single layer and a planar crack-like delamination with a sharp crack tip is not likely to be produced. However, because composite aircraft structure will be exposed to freeze thaw cycling it was considered worthwhile to examine the problem carefully to ascertain whether it should be of concern. Thus the work discussed in Section 3 was undertaken.

1X01674-1

1X01674-2

1X01674-10

1X01674-12

1X01618-3   1X01618-5   1X01618-8   1X01618-16

½ in. NDI Standard   ¼ in. NDI Standard
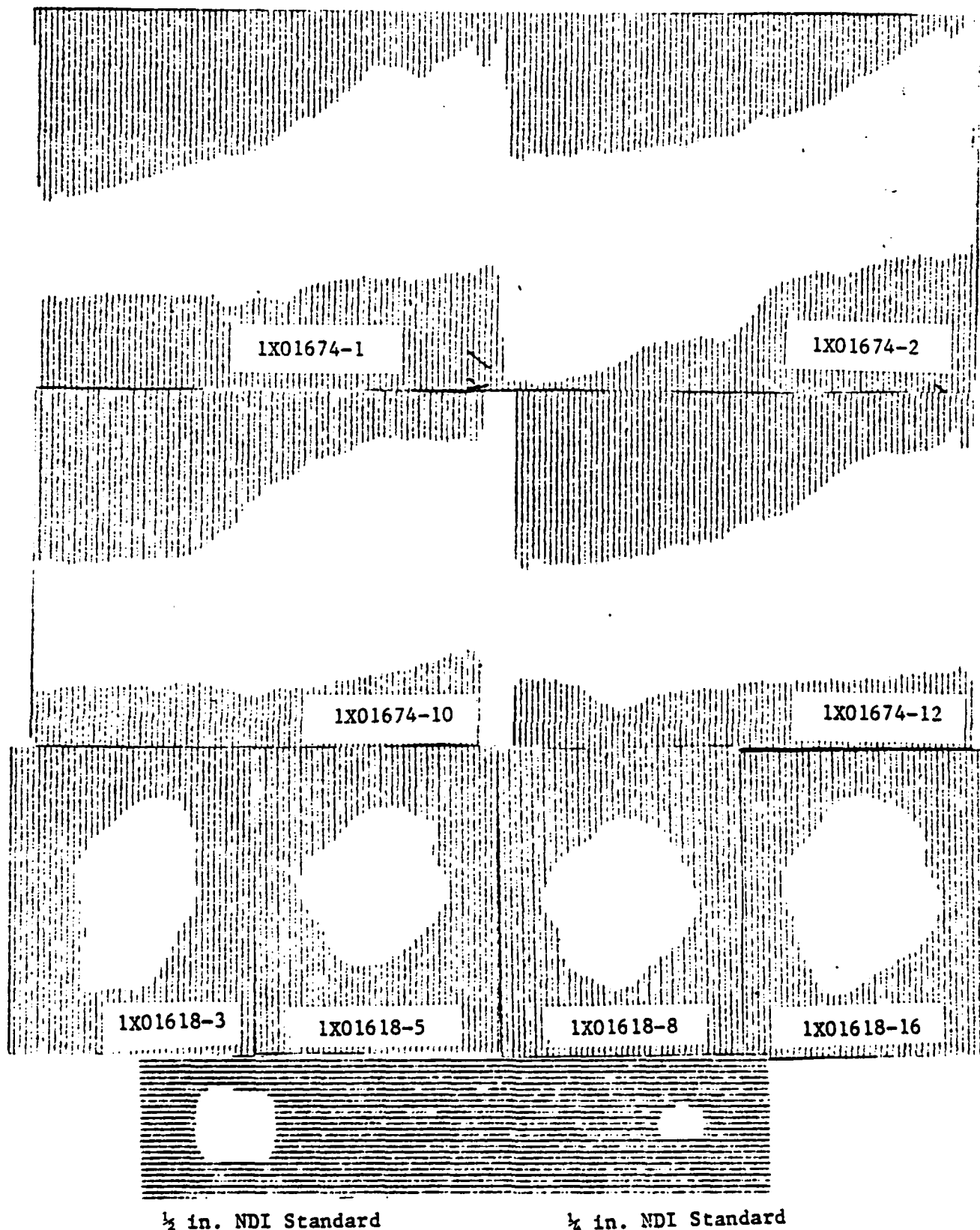
Figure 2.7:   C-Scans After Ninty-nine One Hour
              Cycles of Alternating 160°F
              Immersion with -65°F Exposure

14

SECTION 3
CRACK GROWTH EVALUATION

The task of evaluating crack growth was designed to examine experimentally the likelihood that freeze-thaw cycling can extend delaminations initially present as a result of low velocity impact in a graphite/epoxy laminate by testing coupons which might be representative of a worst case condition. The worst case condition was assumed to be damage for which the entire projected c-scan area would be located on one layer extending the full width of the coupon with no reduction in stiffness of the outer layers. Perhaps a more severe case would be one wherein the damage is completely confined. However, this condition presents formidable experimental difficulties. The specific intent was to determine whether the force required to grow the delamination would exceed that which could conceivably be produced by the 4% expansion of water present in a delamination region as it freezes to ice.

Graphite/epoxy specimens were fabricated from AS/3501-6 prepreg material. Material receiving inspection data and details of panel fabrication are presented in Appendix A. The 1.5 in. x 10.5 in. specimens contained intentional delaminations which were introduced during fabrication by inserting release film (Air Tech. International Inc., A4000 Film) in one of two locations in the 32 ply laminate of the following stacking sequence $(45/0/-45/0/45/0/-45/90)_{2s}$. The film extended the full width of the specimen so the growth of the debond would be easily visible. Six specimens for each of the two debond locations were tested. Debond locations were between the 3rd and 4th plies (-45/0) from the surface and the 7th and 8th plies (-45/90). These debond locations were selected as most nearly representative of the locations in which the near back surface damage occurred in the low velocity impact tests of Reference 1. Ashizawa[5], also reported these locations to be the most critical flaw sites.

Nondestructive ultrasonic inpsection was conducted prior to the cutting of the cured laminate. The only indications were in the locations of the intentional delaminations. Resin and void content measurements were also made. These results are available in Appendix A.

A preliminary study was conducted to select the most viable loading techniques. The two methods illustrated in Figure 3.1 were evaluated. Test set-up and instrumentation for loading methods A & B are shown in Figures 3.2 and 3.3, respectively. Crack displacement was measured, front and back with linear variables differential transformers (LVDT's) in Method A while clip gages were used on both sides for Method B. Type A coupons contained two strips of release film located symmetrically from the outer surfaces to proclude eccentricity in the coupons. Both 1 mil and 1/2 mil thick films were evaluated in Type A coupons. Type B specimens contained only one strip of 1 mil thick release film. The compressively loaded Type A specimens were supported with 1/4-inch thick aluminum plates extending to within 1/2 inch of the initial delamination. Additional support could not be provided without clamping over the delaminated region. Slow crack growth could not be obtained with the Type A loading condition for either film thickness. Despite several modifications of the support fixture, no significant displacement was recorded or observed prior to the sudden and catastrophic failure. With the Type B loading condition slow crack growth could be obtained. However, considerable effort was expended in attempts to obtain uniform opening across the width of the coupon and to obtain more than one data point per coupon. Fairly uniform crack opening displacement (COD) was finally achieved through the use of hydraulic grips and testing under stroke control. This prevented sudden loss of the coupon due to rapid crack extension after the first "pop". Thus multiple COD readings at which crack growth occurred could be taken for various initial crack lengths and displacements. Therefore, the Type B specimen and loading method were selected for all subsequent tests. Crack lengths and displacements on both sides of the specimen were monitored as well as the load to produce extension for a given crack length. Crack lengths were measured with an
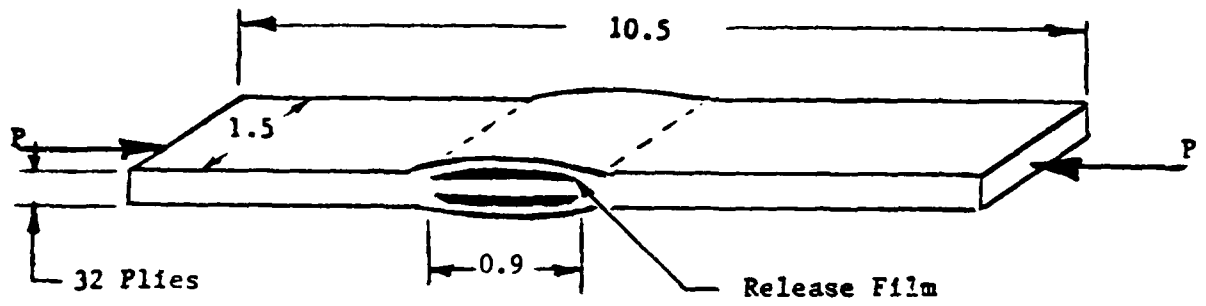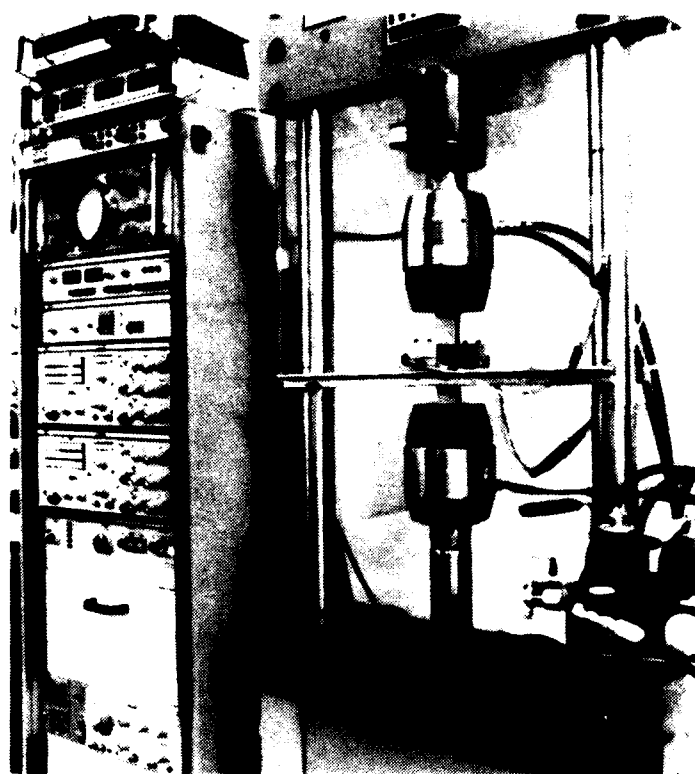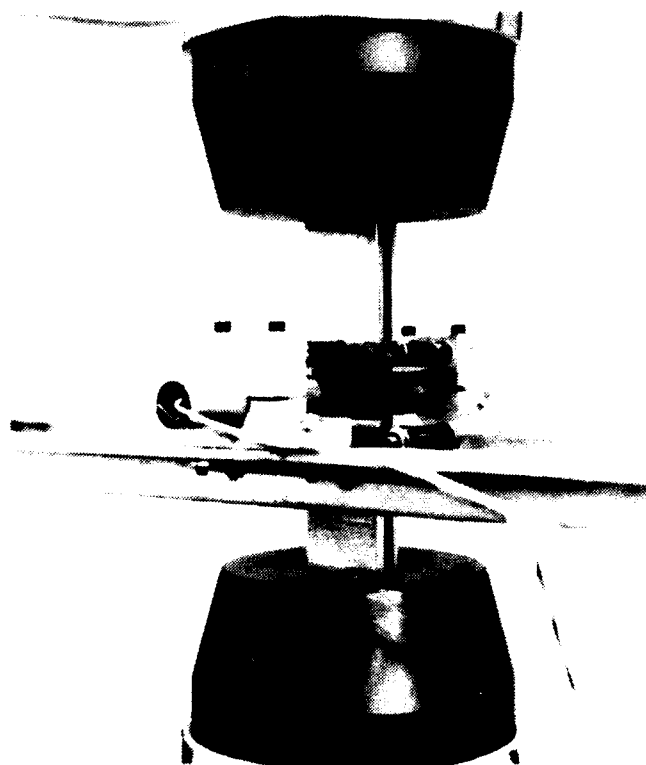
METHOD A
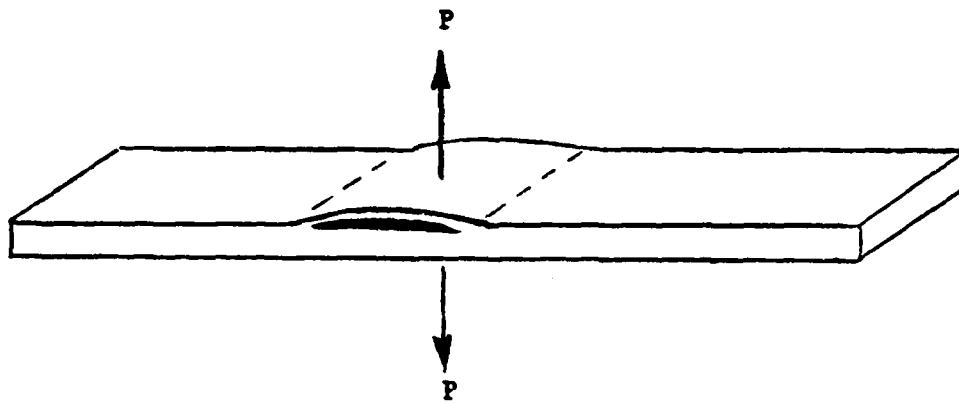
METHOD B

Figure 3.1: Specimen Loading Methods

17

146105R

146106R

Figure 3.2: Test Set-up and Instrumentation For Method A

18
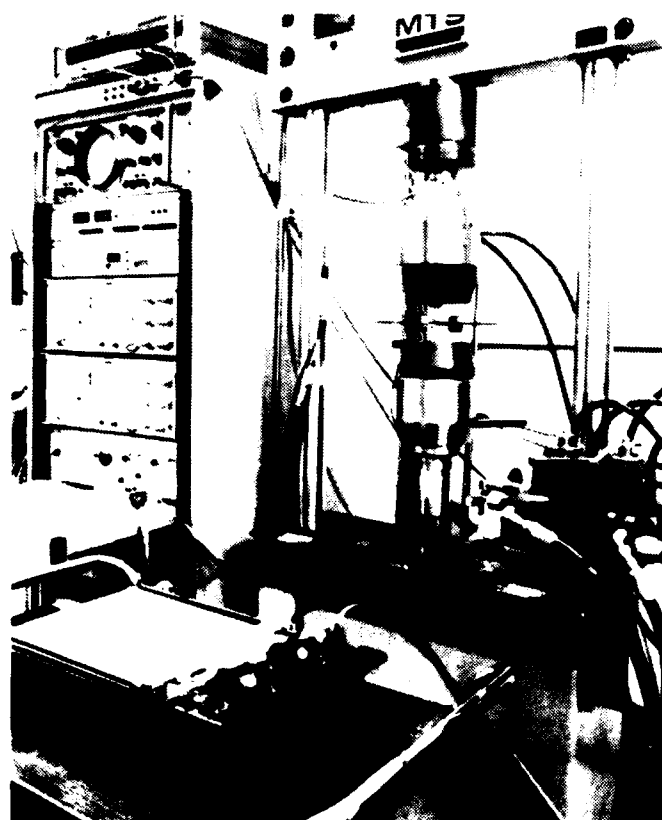
DA9228
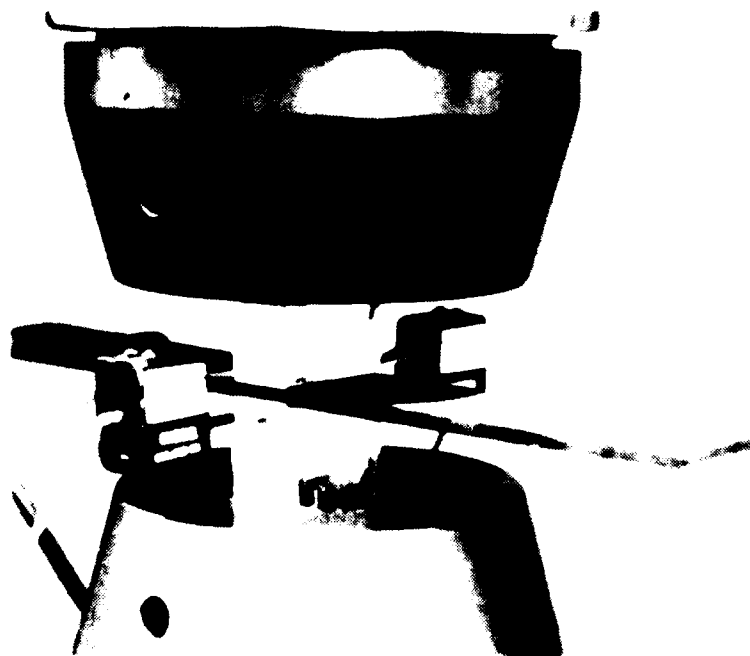
Figure 3.3: Test Set-Up and Instrumentation for Method B

19

optical microscope mounted on the test machine because of the difficulty in seeing the crack tip under no load, a small load (approximately 25% of maximum load) was maintained while the crack length was read. Selected results for specimens with a debond between the 7th and 8th plies (2YXX-1) and those with a debond between the 3rd and 4th plies (1YXX-4) are presented in Figures 3.4 through 3.8 and Figures 3.9 through 3.11, respectively. Table 3.1 contains a tabulation of the complete test results.

The test results indicate that the amount of additional deflection required to propagate the crack is at a minimum equal to the initial deflection and can be as much as seven times the initial deflection.

Consider a typical case where the crack-tip to crack-tip length is one inch, and the crack opening at no load is about 0.001 inch. The crack is not extended by transverse loading until the opening is increased elastically to about 0.003 inch. Assume that the crack shape at no load is geometrically similar to that when loaded -- that is; all ordinates bear a 0.001/0.003 relation.

Consider:

1. If the crack at no load fills completely with water, which freezes uniformly with no escape, all crack ordinates must increase by four percent.

2. The geometry is well within the realm of linear small deflection theory, and the crack expanded four percent by freezing will have the same contour it would have if it were opened up by applying transverse load, sufficient to increase the opening at the center from 0.00100 to 0.00104 inch.

3. Since the crack will not run until the opening is increased at least fifty times this much, freeze-thaw effects do not appear to be capable oof producing delamination growth.

This conclusion is weakened by the assumption that the unloaded crack has the same contour shape as the crack under load. It seems probable that at

NADC METHOD B
TEST 20244 RUN 2
Y-AXIS CH 47   YMAX = .2296E 03 YMIN = -.2083E 02
X-AXIS CH 48   XMAX = .1282E-02 XMIN = -.9142E-04

13:39 09/20/82

2YXX-1, FRONT, 1ST LOAD

Figure 3.4a: Load vs. Crack Opening Displacement for Initial COD of 0.0001 in. and Initial
Crack Length of 0.9 in. - Front Gage

21

NADC METHOD B
TEST 20244 RUN 2

13:39 09/20/82

Y-AXIS CH 47   YMAX = .2296E 03   YMIN = -.2083E 02
X-AXIS CH 49   XMAX = .1629E-02   XMIN = -.1280E-03

2YXX-1, REAR, 1ST LOAD

Figure 3.4b: Load vs. Crack Opening Displacement for Initial COD of 0.0001 in. and Initial Crack
Length of 0.9 in. - Rear Gage

Figure 3.5a: Load vs. Crack Opening Displacement for Initial COD of 0.001 in. and Initial Crack Length of 1.016 in. - Front Gage

Figure 3.5b: Load vs. Crack Opening Displacement for Initial COD of 0.0001 in. and Initial
Crack Length of 1.025 in. -- Rear Gage

NADC METHOD B
TEST 20256   RUN 1

10:30 09/21/82

Y-AXIS CH 47   YMAX = .1767E 03 YMIN = -.2514E 02
X-AXIS CH 48   XMAX = .6189E-02 XMIN = -.2928E-03

2YXX-1, FRONT, 8TH LOAD

Figure 3.6a: Load vs. Crack Opening Displacement for Initial COD of 0.001 in. and Initial Crack
Length of 1.231 in. - Front Gage

Figure 3.6b: Load vs. Crack Opening Displacement for Initial COD of 0.001 in. and Initial Crack Length of 1.200 in. - Rear Gage.
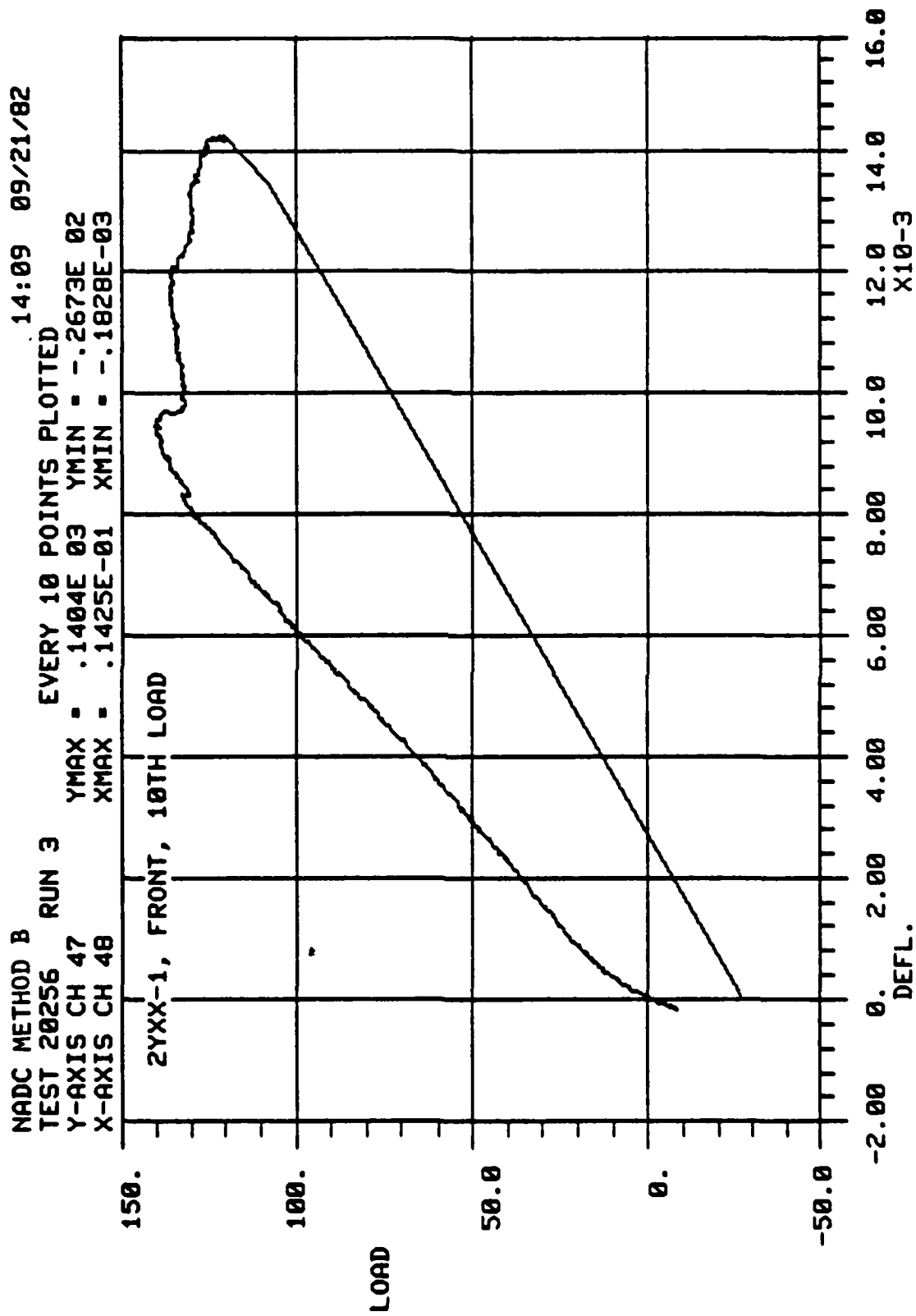
Figure 3.7a: Load vs. Crack Opening Displacement for Initial COD of 0.0013 in. and Initial Crack Length of 1.532 in. – Front Gage
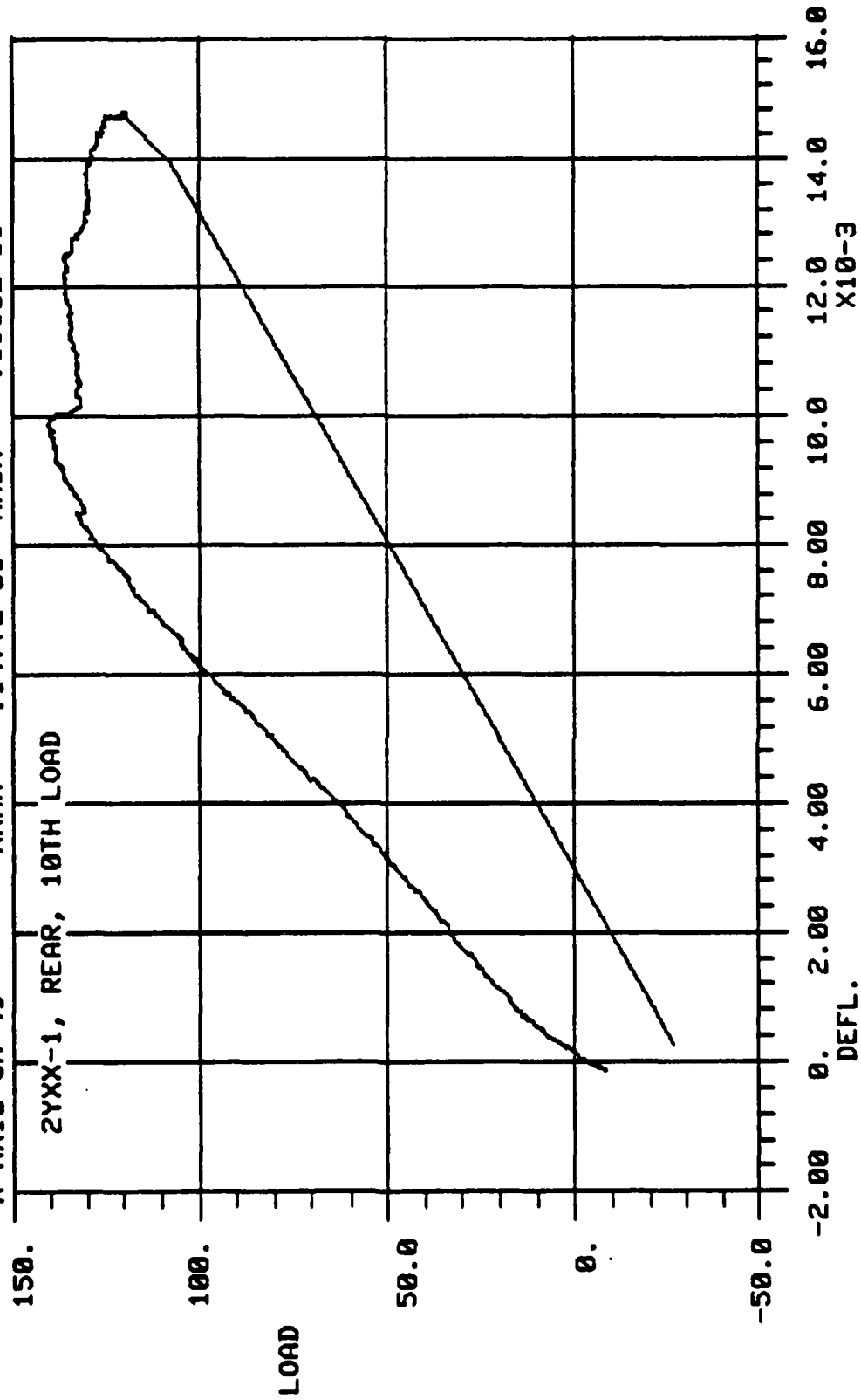
Figure 3.7b: Load vs. Crack Opening Displacement for Initial COD of 0.0019 in. and Initial Crack Length of 1.746 in. - Rear Gage
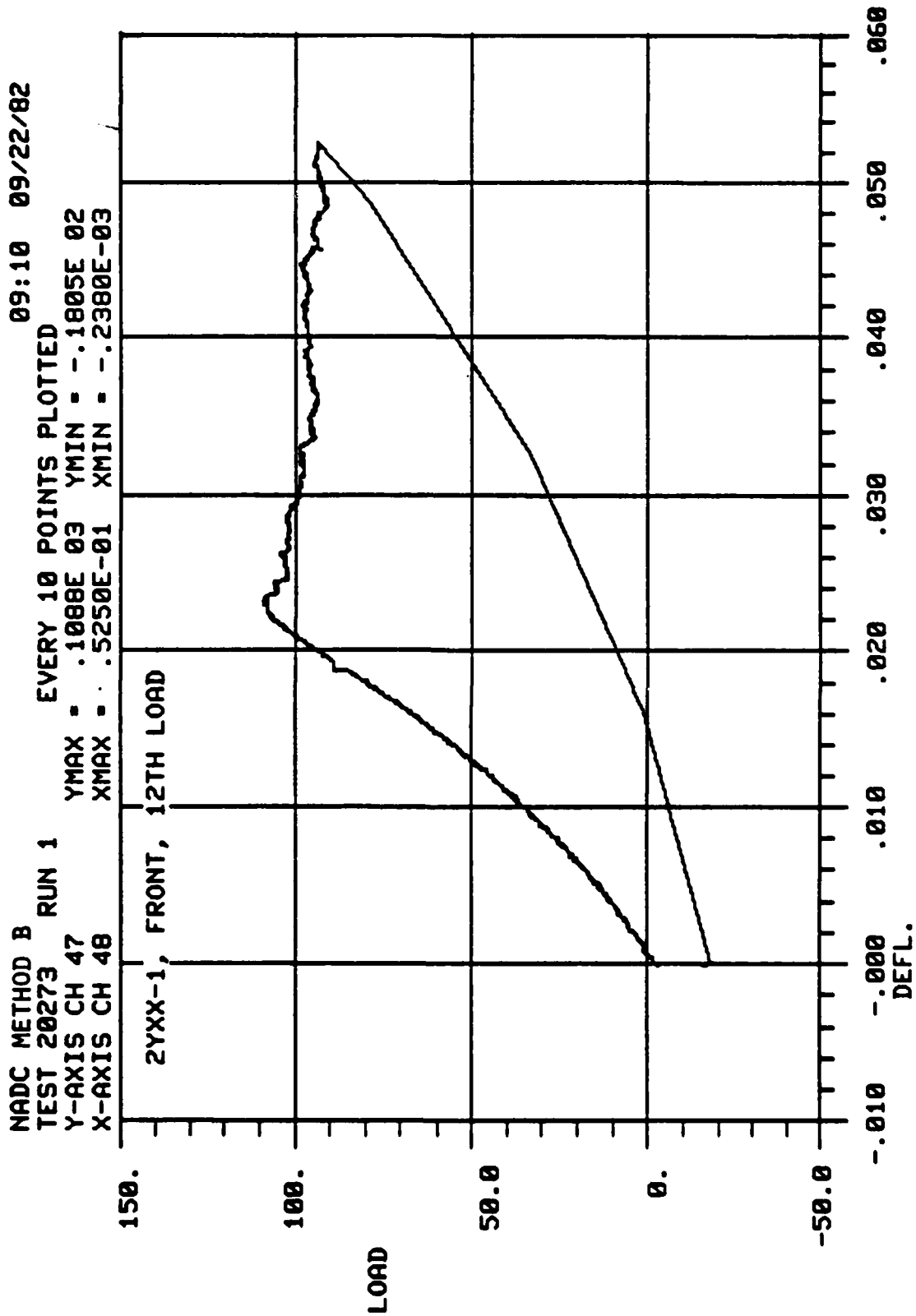
Figure 3.8a: Load vs. Crack Opening Displacement for Initial COD of 0.0026 in. and Initial Crack Length of 2.060 in. - Front Gage

Figure 3.8b: Load vs. Crack Opening Displacement for Initial COD of 0.0026 in. and Initial Crack Length of 1.900 in. - Rear Gage
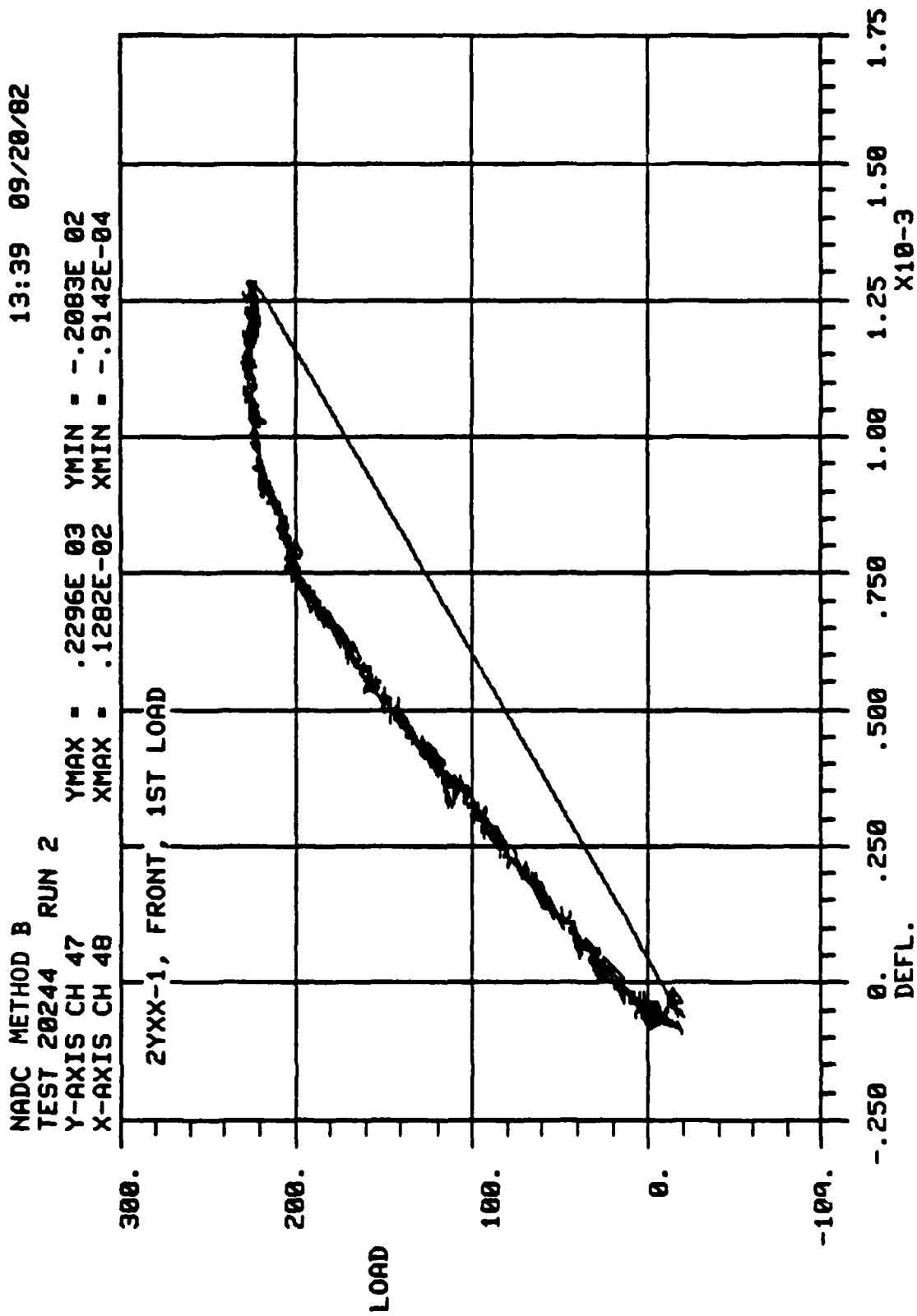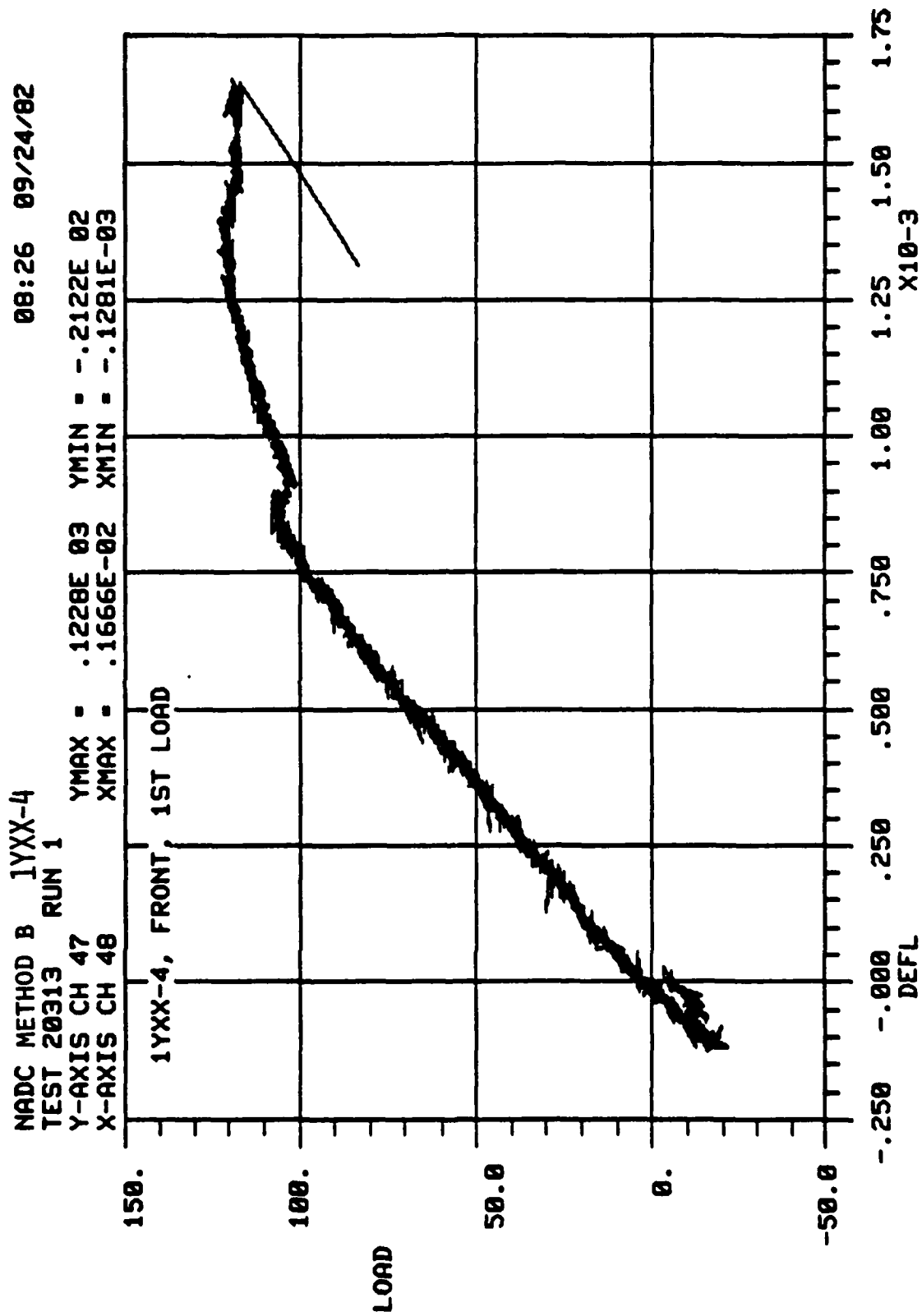
Figure 3.9a: Load vs. Crack Opening Displacement for Initial COD of 0.001 in. and Initial Crack Length of 0.9 in. - Front Gage
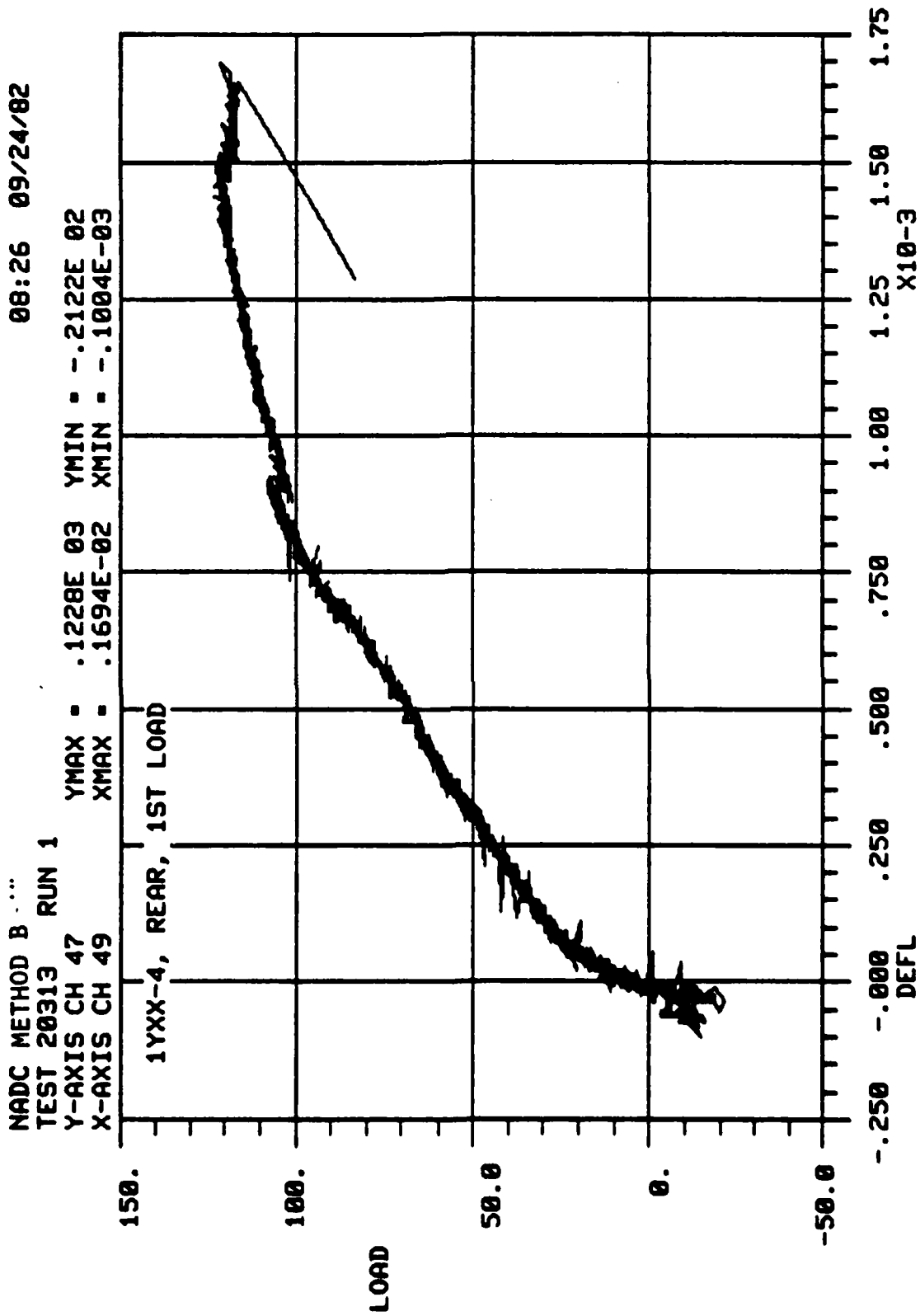
Figure 3.9b: Load vs. Crack Opening Displacement for Initial COD of 0.001 in. and Initial Crack Length of 0.9 in. - Rear Gage
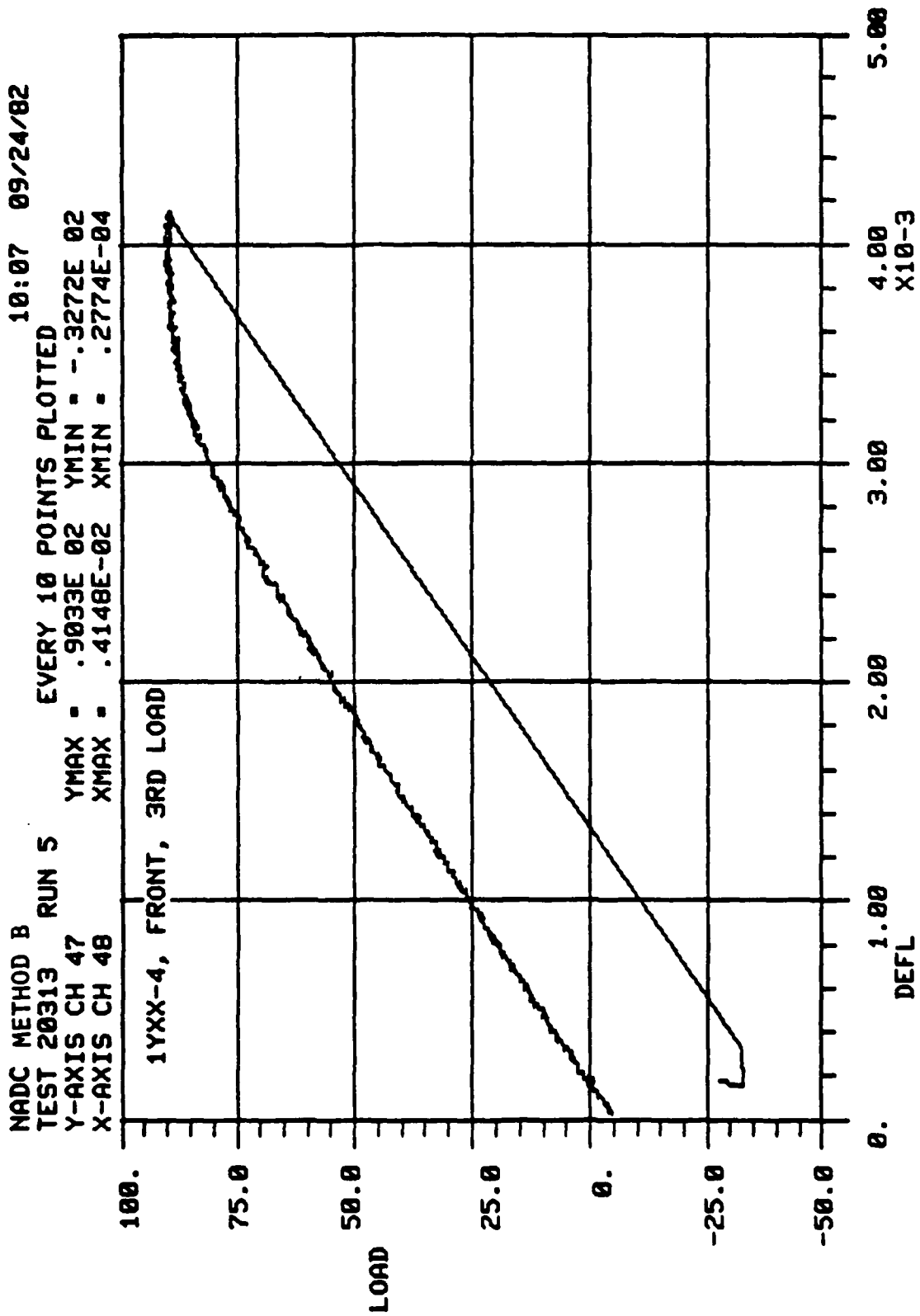
Figure 3.10a: Load vs. Crack Opening Displacemtn for Initial COD of 0.0013 in. and Initial Crack
Length of 1.015 in. - Front Gage
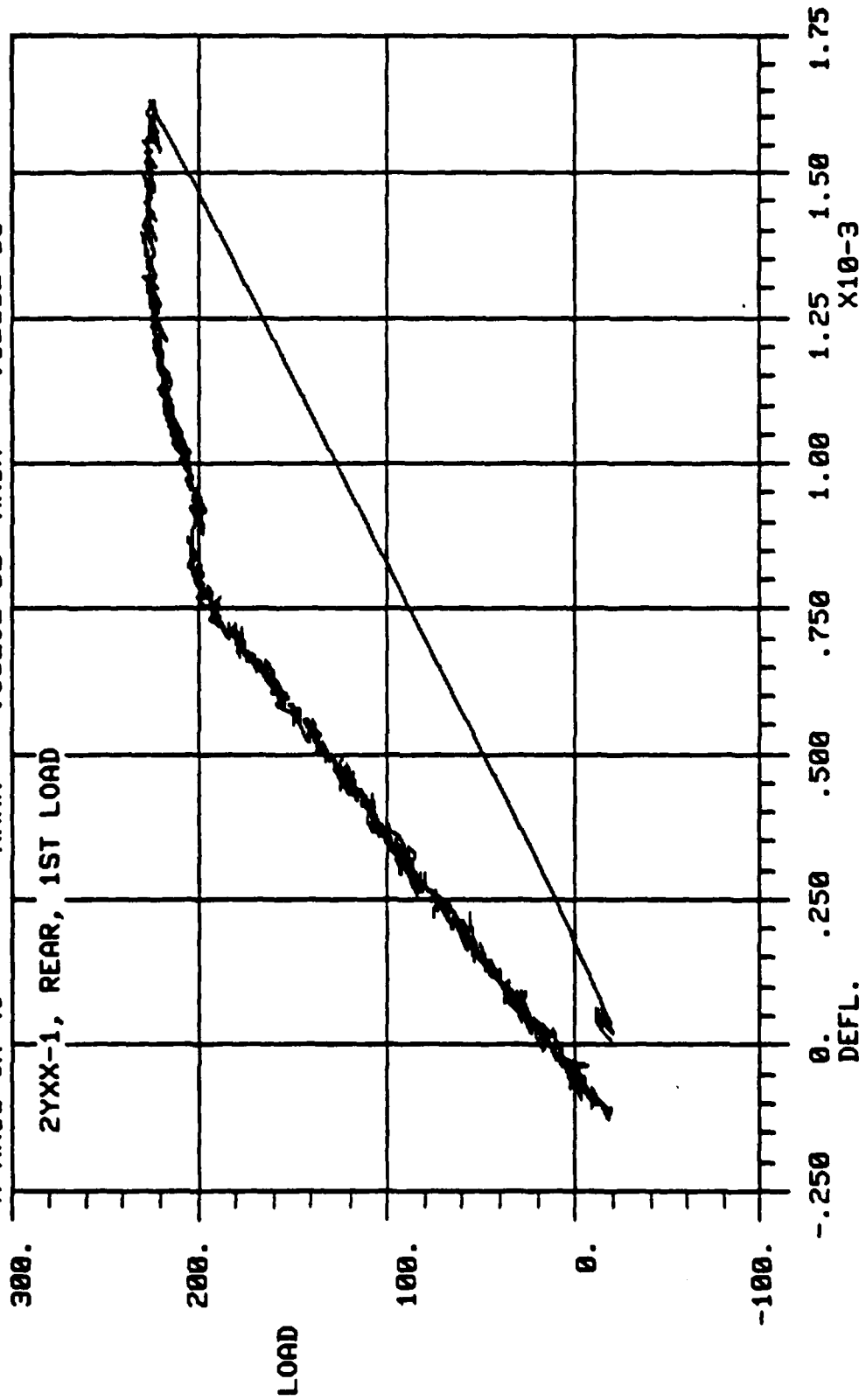
Figure 3.10b: Load vs. Crack Opening Displacement for Initial COD of 0.0013 in. and Initial Crack Length of 0.985 in. - Rear Gage

NADC METHOD B
TEST 20313   RUN 9   EVERY 10 POINTS PLOTTED
Y-AXIS CH 47   YMAX = .8557E 02 YMIN = -.4517E 01
X-AXIS CH 48   XMAX = .1509E-01 XMIN = -.8949E-05

TYXK-4, FRONT, 5TH LOAD
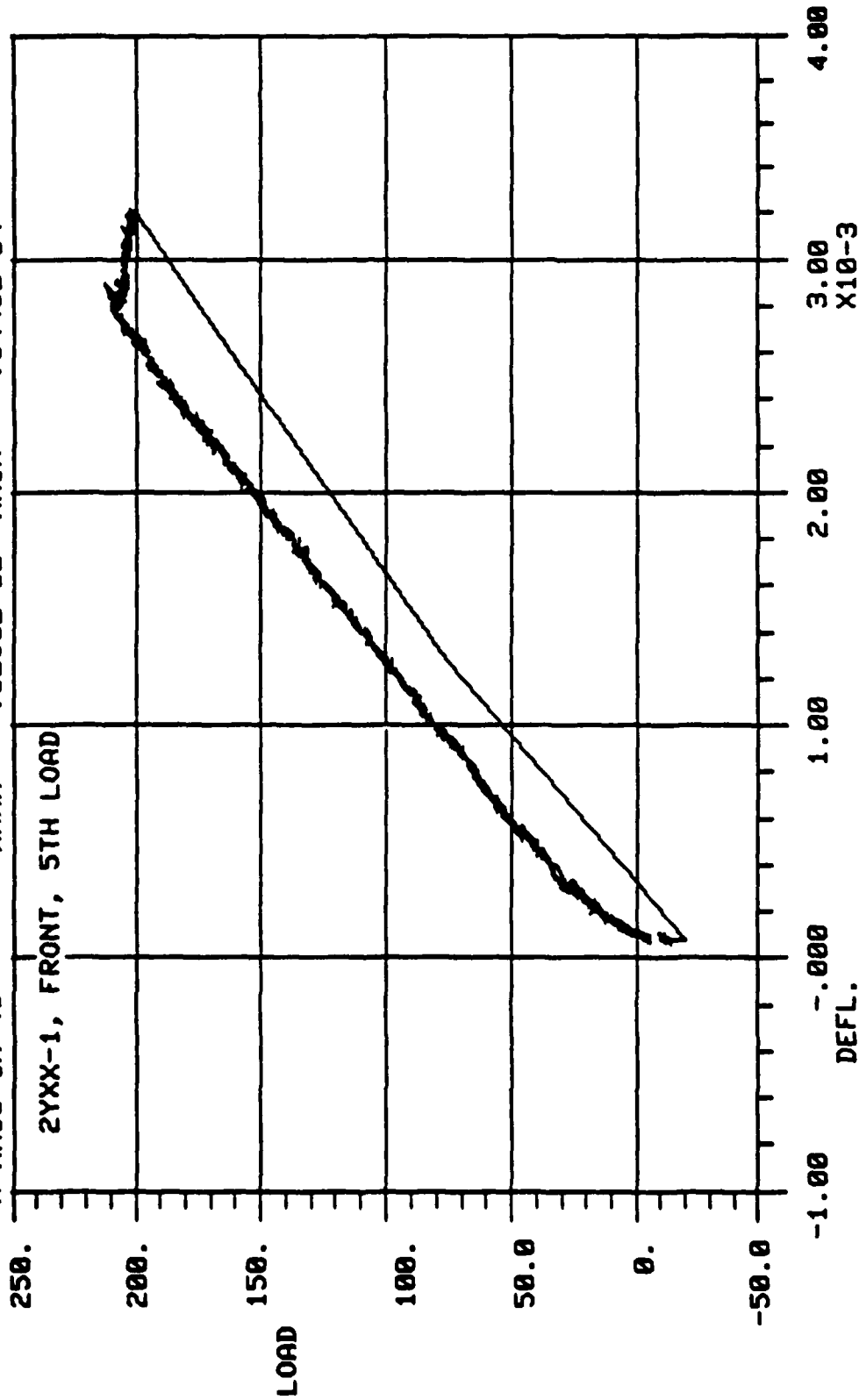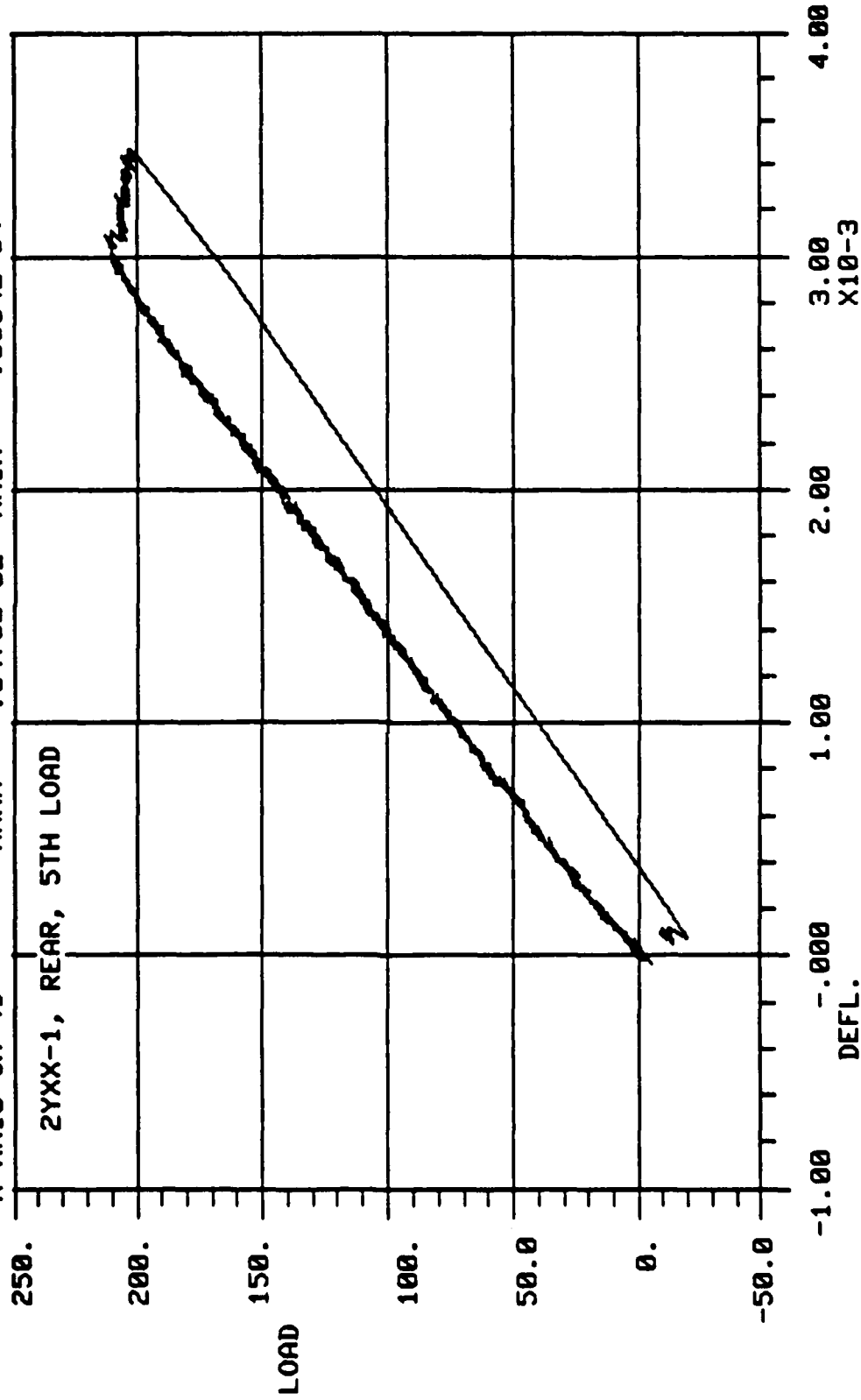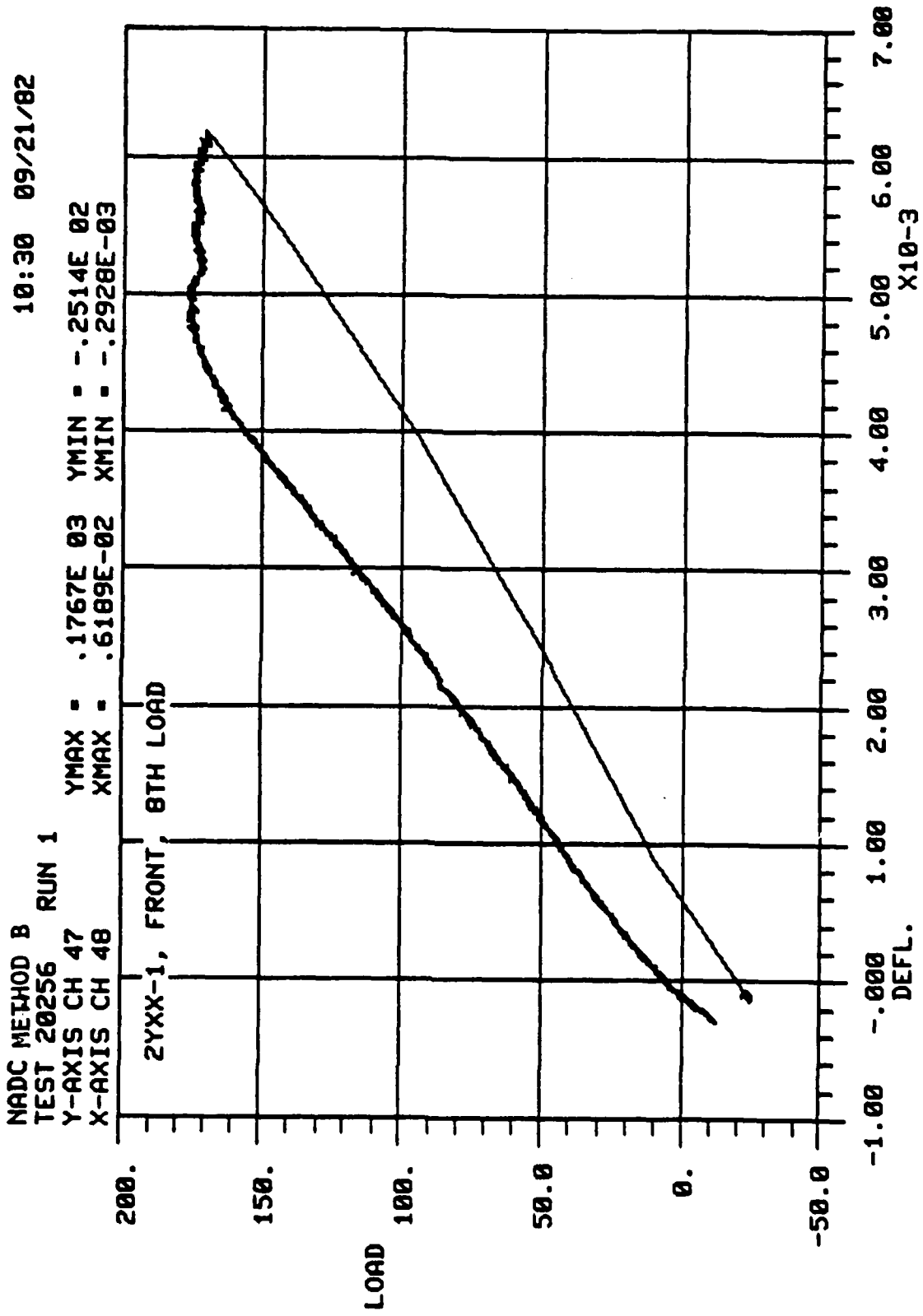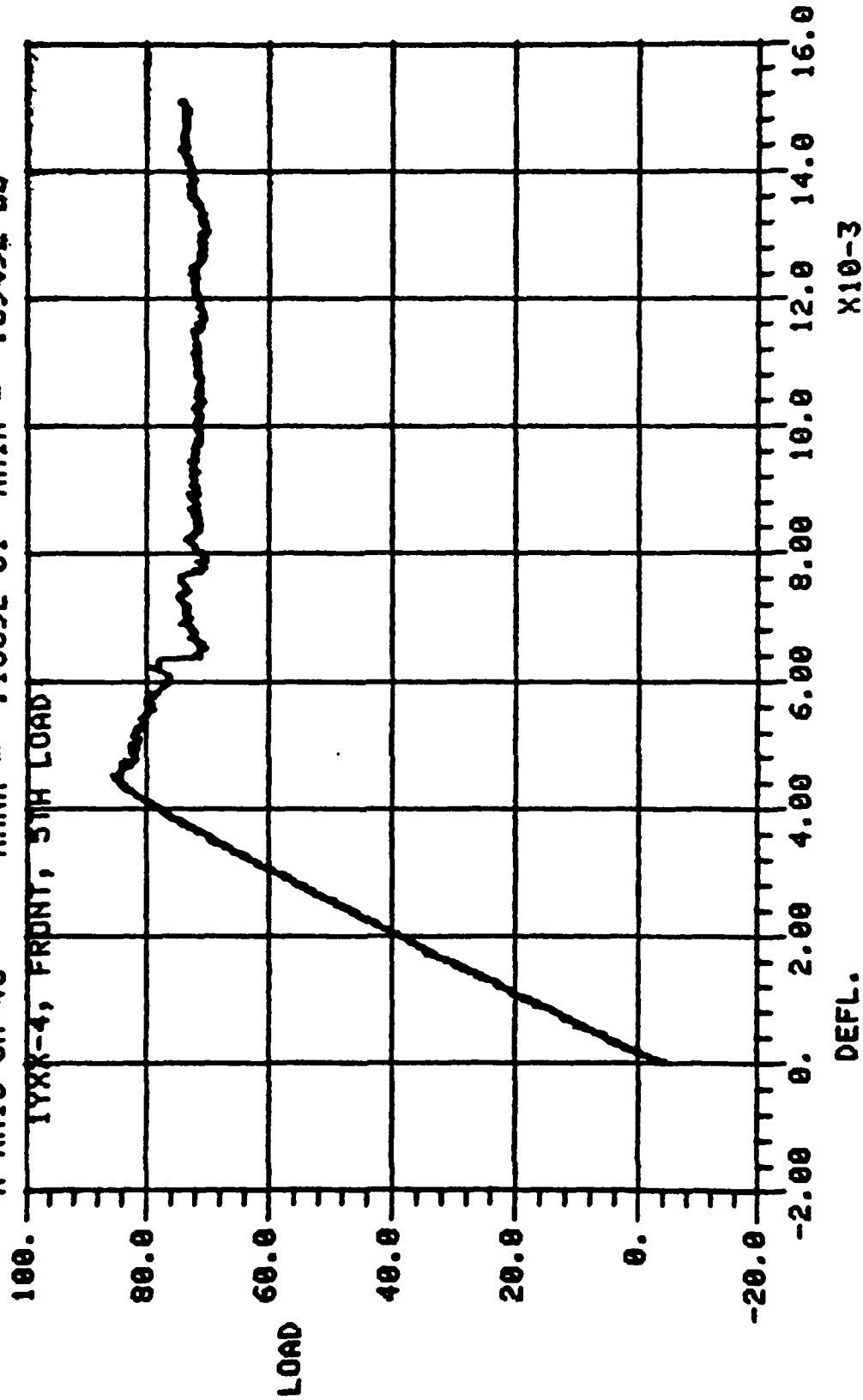
Figure 3.11a: Load vs. Crack Opening Displacement for Initial COD of 0.0016 in. and Initial
Crack Length of 1.125 in. - Front Gage

35
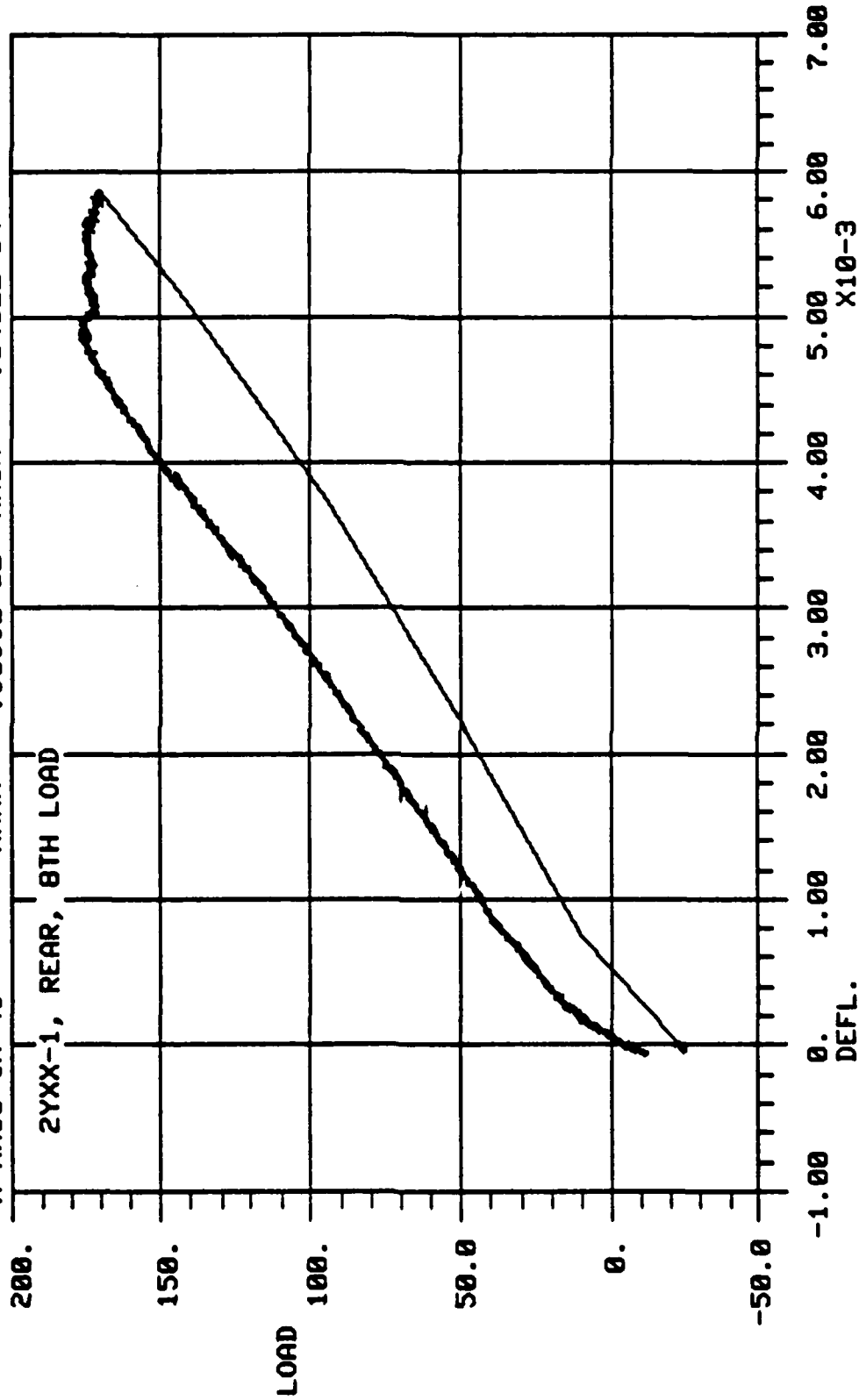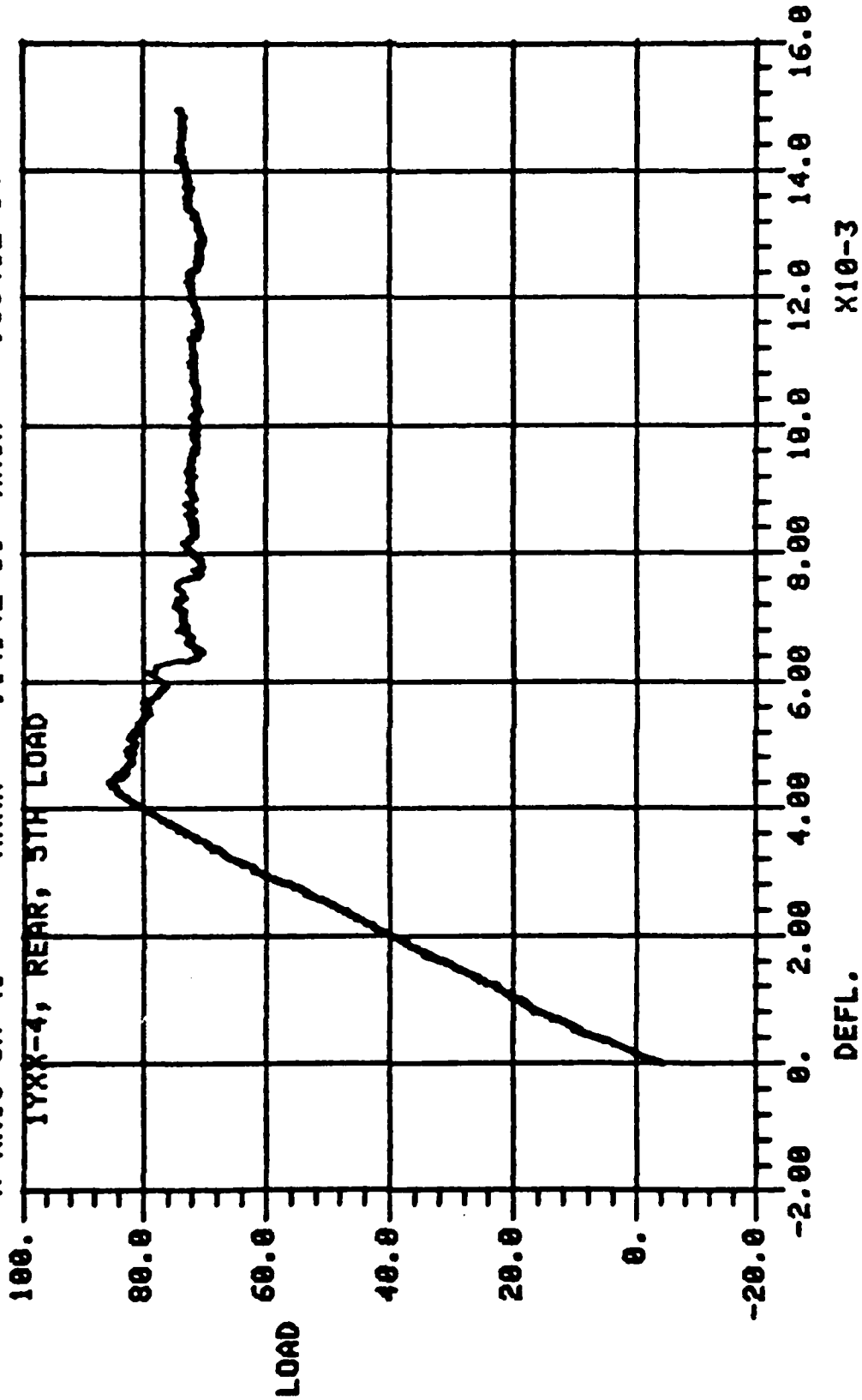
Figure 3.11b: Load vs. Crack Opening Displacement for Initial COD of 0.0016 in. and Initial Crack Length of 1.000 in. - Rear Gage

TABLE 3.1

TEST RESULTS FOR METHOD B LOADING

(See Figure 3.1)

Specimen ID	Max Load lbs	Initial COD (in.) Front	Initial COD (in.) Rear	Initial Crack Length (in.) Front	Initial Crack Length (in.) Rear	Additional COD @ "POP" (in.) Front	Additional COD @ "POP" (in.) Rear	Controlled Fcn	Grips
1YXX-1	-	.001	.001	.9	.9	-	-	Stroke	Hydraulic
	122	.0014	.0012	1.100	.893	.00183	.00168		
	107	.0014	.0012	1.142	.918	.0026	.0024		
	77	.0029	.0027	1.212	1.046	.0070	.0069		
1YXX-2	120	.001	.001	.9	.9	.00095	.0012	Stroke	Hydraulic
	112	.0012	.0013	.9	.9	.00163	.0017		
	106	.0013	.0014	1.013	.946	.0027	.0027		
	80	.0026	.0025	1.148	1.049	.0072	.0072		
1YXX-3	149	.001	.001	.9	.9	.0015	.0008	Stroke	Hydraulic
	148	.001	.001	.9	.9	.00168	.0010		
	130	.0012	.0012	.953	.941	.0024	.0018		
	78	.0030	.0028	1.105	1.075	.0065	.0064		
1YXX-4	123	.001	.001	.9	.9	.00125	.00125	Stroke	Hydraulic
	119	.001	.001	.953	.9	.00145	.00156		
	90	.0013	.0013	1.015	.985	.0034	.0034		
	89	.0018	.0017	1.122	1.000	.0040	.0040		
	86	.0016	.0016	1.125	1.000	.0044	.0044		

TABLE 3.1-(Continued)
TEST RESULTS FOR METHOD B LOADING

Specimen ID	Max Load lbs	Initial COD (in.) Front	Rear	Initial Crack Length (in.) Front	Rear	Additional COD @ "POP" (in.) Front	Rear	Controlled Fcn	Grips
1YXX-5	211	.001	.001	.898	.896	–	.0023	Load	Pinned
	102	.001	.001	–	–	.082	.087		
	99	.023	.019	2.201	2.421	.050	.050		
	76	.024	.031	2.860	2.602	.058	.058		

LOST COUPON FIRST LOADING

Specimen ID	Max Load lbs	Initial COD (in.) Front	Rear	Initial Crack Length (in.) Front	Rear	Additional COD @ "POP" (in.) Front	Rear	Controlled Fcn	Grips
1YXX-6									
2YXX-1	230	.001	.001	.9	.9	.001	.0012	Stroke	Hydraulic
	228	.001	.001	0.930	0.906	.0013	.0016		
	222	.001	.001	–	–	.0016	.00168		
	214	.001	.001	1.008	.969	.0023	.0026		
	212	.001	.001	1.016	1.025	.0028	.0030		
	201	.001	.001	–	–	.0033	.0035		
	192	.001	.001	1.092	1.135	.0039	.0045		
	177	.001	.001	1.231	1.200	.0048	.0049		
	170	.001	.001	1.343	1.327	.006	.0061		
	140	.0013	.002	1.532	1.746	.0096	.0099		
	125	.0025	.0029	1.675	1.900	.0135	.0135		
	109	.0036	.00 6	2.060	2.584	.023	.023		
	96	.01 2	.01 3	2.504		.044	.044		
2YXX-2	217	.001	.001	.9	.9	.00155	.00155	Stroke	Hydraulic
2YXX-3	158	.001	.001	1.337	0.926	.0145	.0035	Load	Hydraulic
	104	.008	.011	2.69	2.43	.064	.064		
2YXX-4	232	.001	.001	–	–	.0016	.002	Load	Hydraulic
2YXX-5	222	.001	.001	.911	.902	.002	.008	Load	
	153	.001	.001	1.079	1.276	.005	.009		
	153	.001	.001	1.268	1.395	.008	.0096		
		.001	.001	1.277	1.446	.0086	.0106		

LOST COUPON FIRST LOADING

no load the crack is being held open by asperities existing close to the crack tip, thus, in the critical region, the reasoning could not apply.

The above results did not completely answer the question; as an additional check another experimental effort was undertaken involving a small number of specimens.

Specimen 1YXX-4 was loaded to a COD of 0.015 in., the maximum deflection at which the crack started to propagate at the last loading. The crack was then wedged open with a wood sliver to maintain this deflection. One side of 1YXX-4 and 1YXX-3, which was not wedged open (COD = 0.006 in.) was sealed with wax. Water was then injected with an hypodermic needle into the cracks of the two specimens and the other side sealed. These specimens were then subjected to 210 cycles of alternating $-65^\circ F$ and $160^\circ F$ temperatures, taking 13 minutes to complete one cycle.

Since the crack tips are very difficult to detect, the specimens were loaded to 50 lbs. while crack lengths were read. Both crack lengths appeared to have increased by about 0.09 inch. However the sample size is small and there is considerable room for experimental error. The cracks may have extended due to the procedure of injecting the water, although a crack length reading was taken after this procedure, but not under load, and a crack length increase could not be detected. The 50 lb. load applied to take the final reading may also have caused the cracks to extend.

Under internal research funding the above experiment was reported a second time with modifications intended to result in more accurate crack measurements. The two previously tested specimens (1YXX-3 & 4) and two additional specimens having comparable crack lengths (1YXX-1 & 2) were prepared by sanding the edges. The crack in Specimen 1YXX-4 was again wedged open to an average COD of 0.015 in. Crack length measurements were made by optical microscope with a 20 lb. load applied to specimens 1YXX-3 & 4 and with no load applied to 1YXX-1 & 2. The apparent locating of the

crack tips were marked on the specimens. Acetate replicas of both specimen edges were then obtained for the four specimens. Water was injected into the cracks. Specimens were sealed and placed in a chamber with alternating -65°F and 160°F temperatures. After 1100 cycles, specimens were removed and edges replicated. Crack length measurements were made in the same manner as prior to the thermocycling. Crack length measurements made by optical microscopy once again indicated a change as shown in Table 3.2. However careful study of the edge replicas appears to indicate no change. Photographs of typical replicas are presented in Figures 3.13 through 3.19. The crack designations employed in these figures are illustrated in Figure 3.12. Cracks are much more clearly visible on the replicas than with direct observation by optical microscopy even with specimens under load. For example, in Figure 3.13 the location of the crack tip as determined by direct optical observation does not appear to coincide with the end of a crack on this replica. This was true for most of the observations. Figures 3.14 through 3.16 illustrate cases where there was good agreement for both methods of detection and for this specimen (1YXX-3) it is fairly clear that there has been no change. Crack tips were much more difficult to discern in the other specimens as shown in Figures 3.17 through 3.19, but in each case at least one specimen edge was readable. Again, these inc ate no change.

Clearly a need still exists to perform experiments comparable to these on much larger sample sizes using some method to mark the crack so it is more clearly visible.

It is also important to note that these experiments represented a very severe condition where moisture was forced to fill the entire crack volume and may not be realistic.

TABLE 3.2
CRACK LENGTH MEASURED BY OPTICAL MICROSCOPY

Specimen ID	Location	Crack Length Prior to Cycling	Crack Length After Cycling
1YXX-1	Front	1.507	1.714
	Rear	1.186	1.247
1YXX-2	Front	1.424	1.473
	Rear	1.448	1.459
1YXX-3	Front	1.677	1.468
	Rear	1.477	1.415
1YXX-4	Front	1.311	1.636
	Rear	1.404	1.621
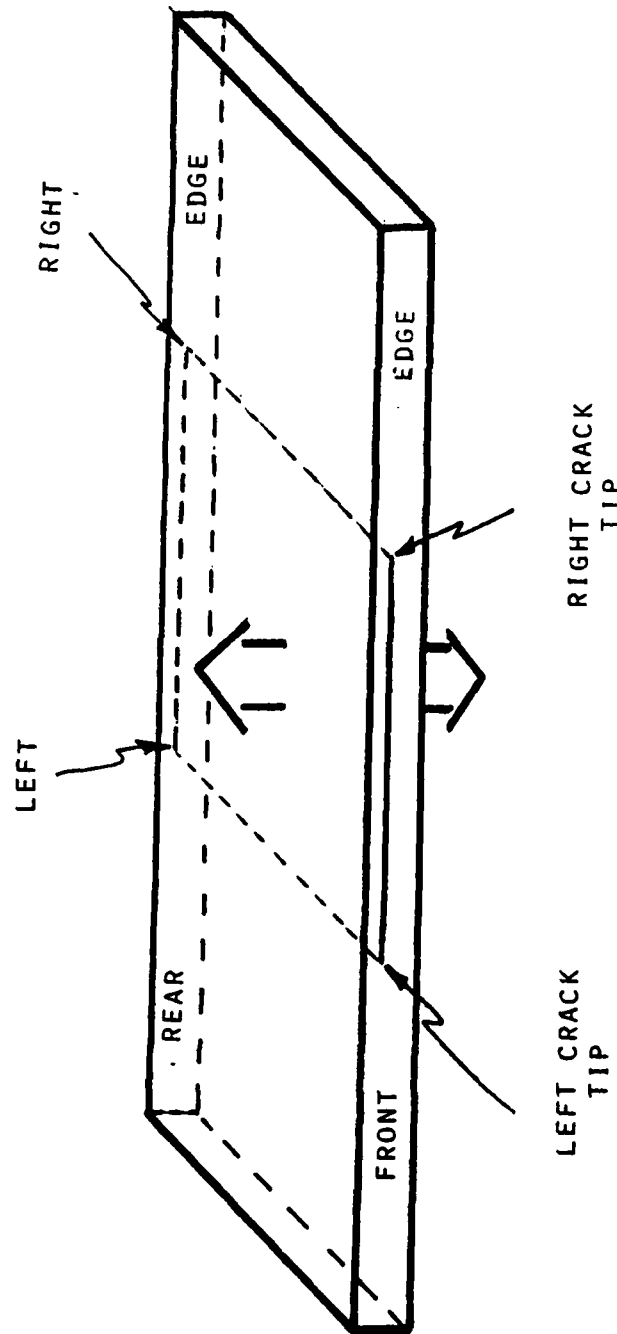
Figure 3.12: Crack Identification Used for Replicas – Figures 3.13 through 3.19.
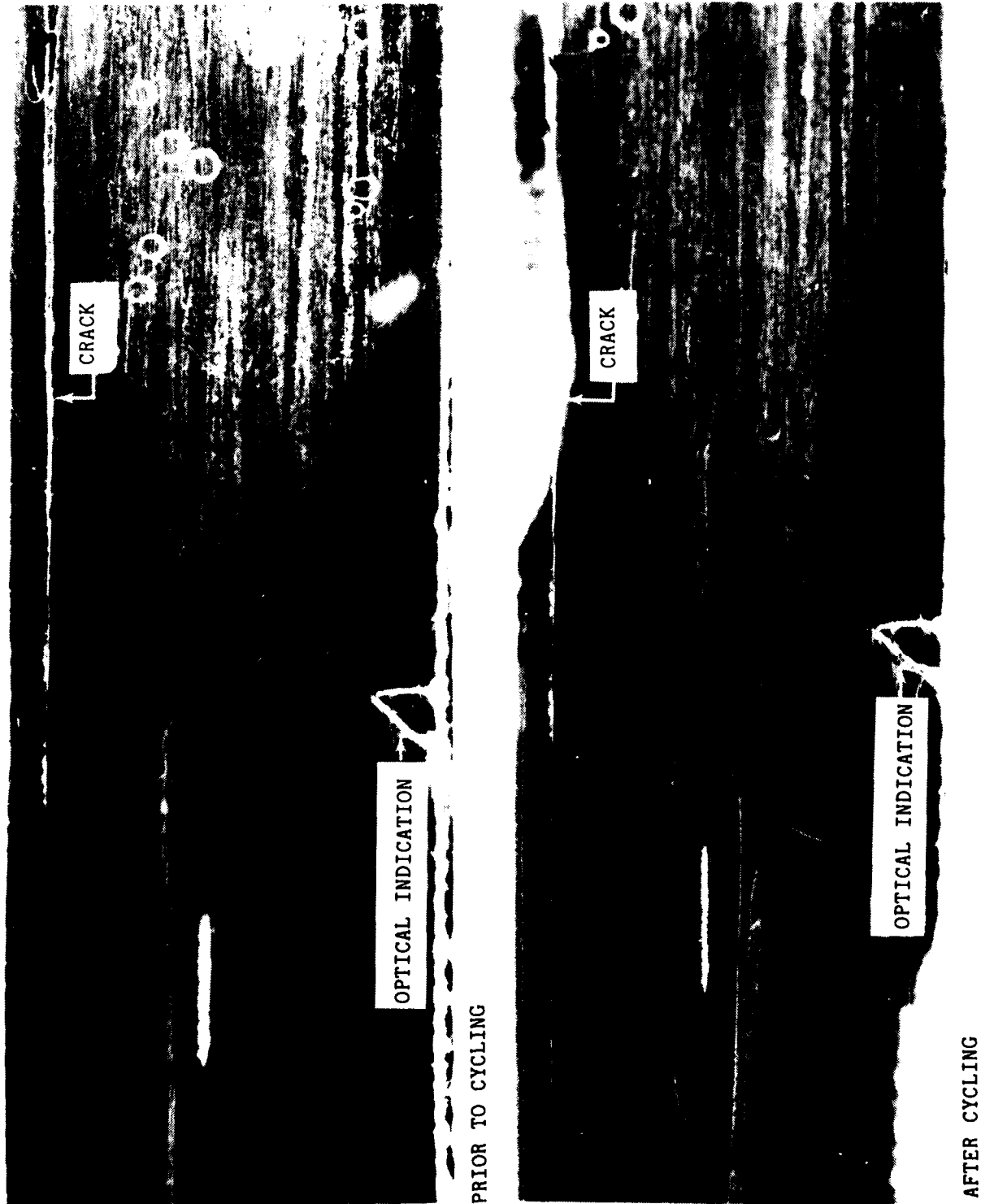
Figure 3.13: Replica of Left Crack Tip Front Edge of Specimen 1YXX-3 Before and After 1100 Thermocycles.
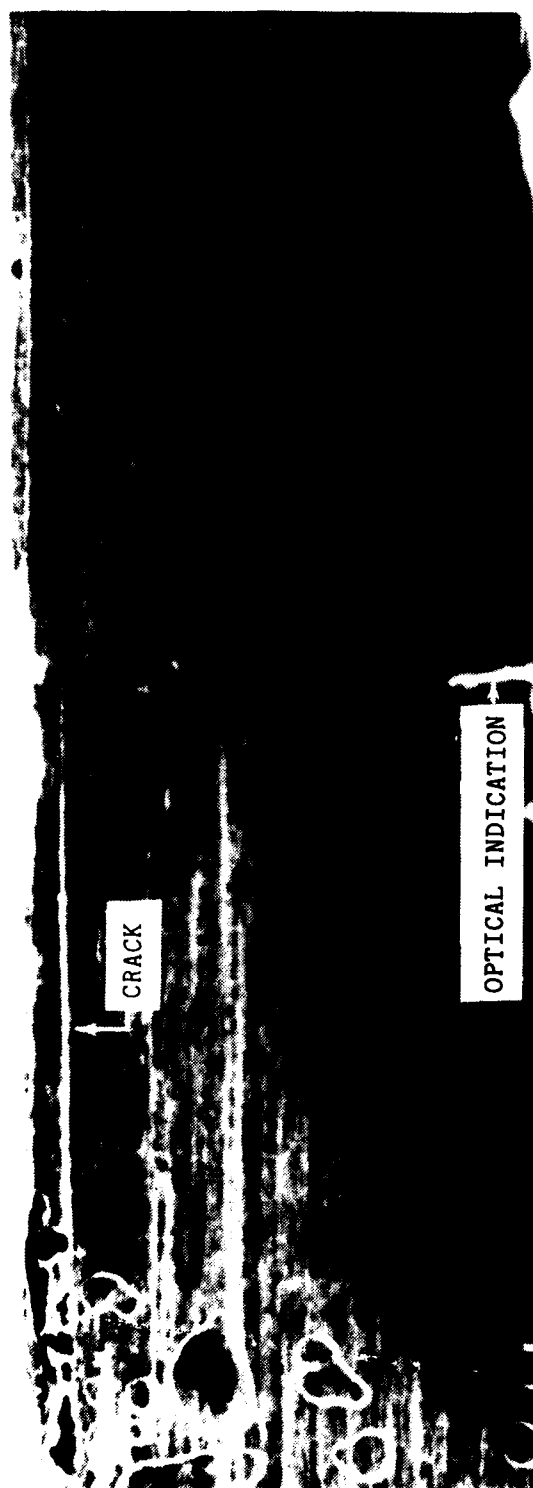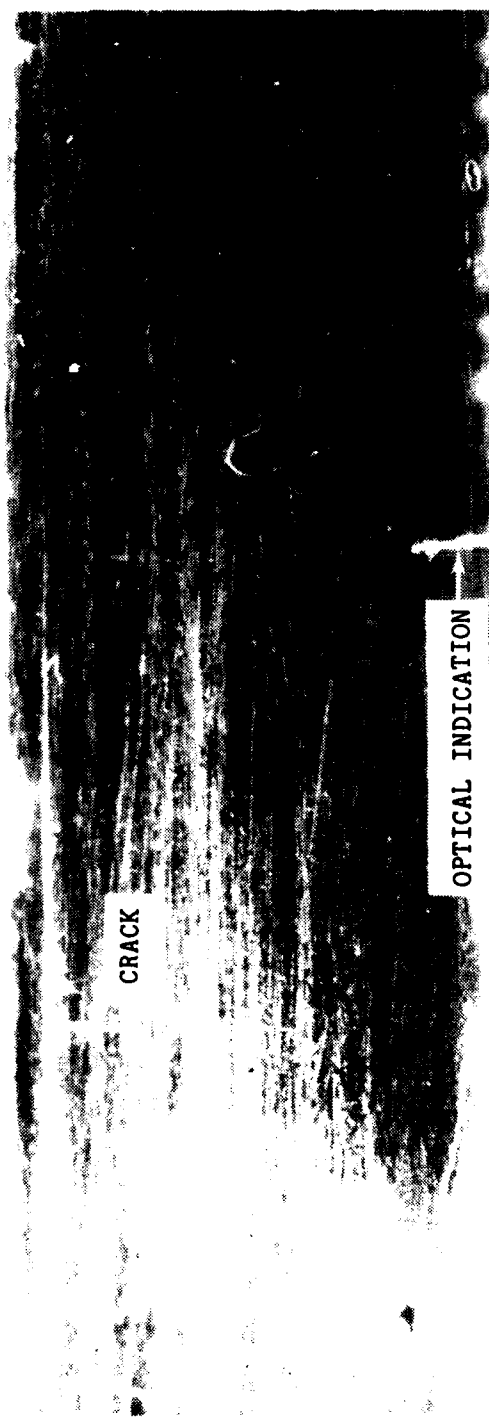
Figure 3.14: Replica of Right Crack Tip Front Edge of Specimen 1YXX-3 Before and After 1100 Thermocycles.

CRACK

OPTICAL INDICATION

PRIOR TO CYCLING

CRACK

OPTICAL INDICATION
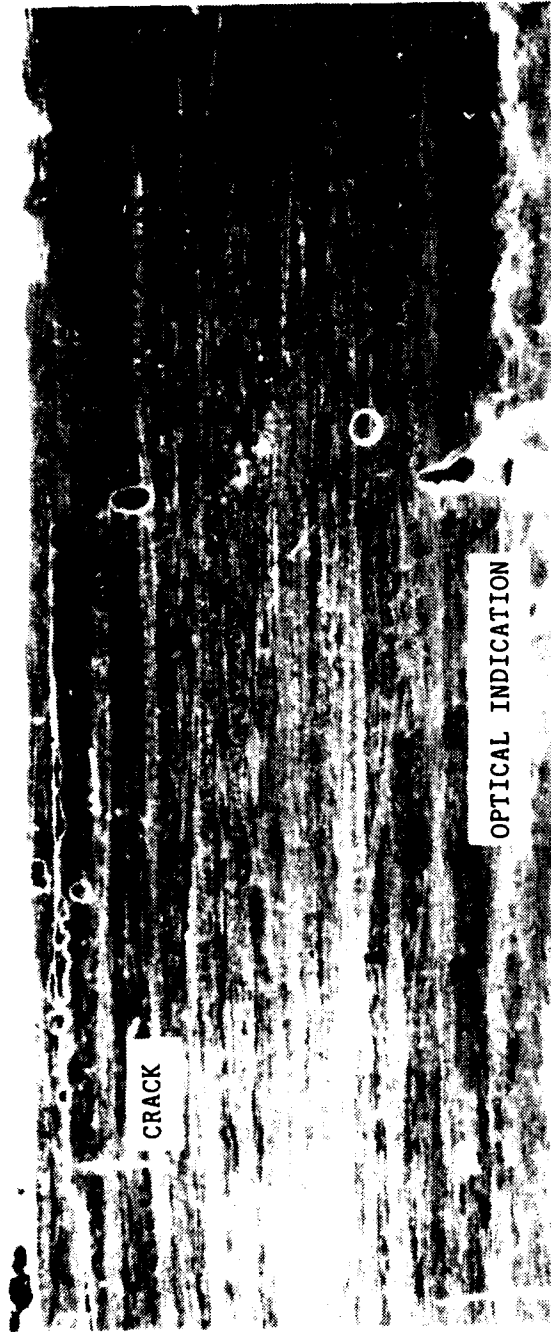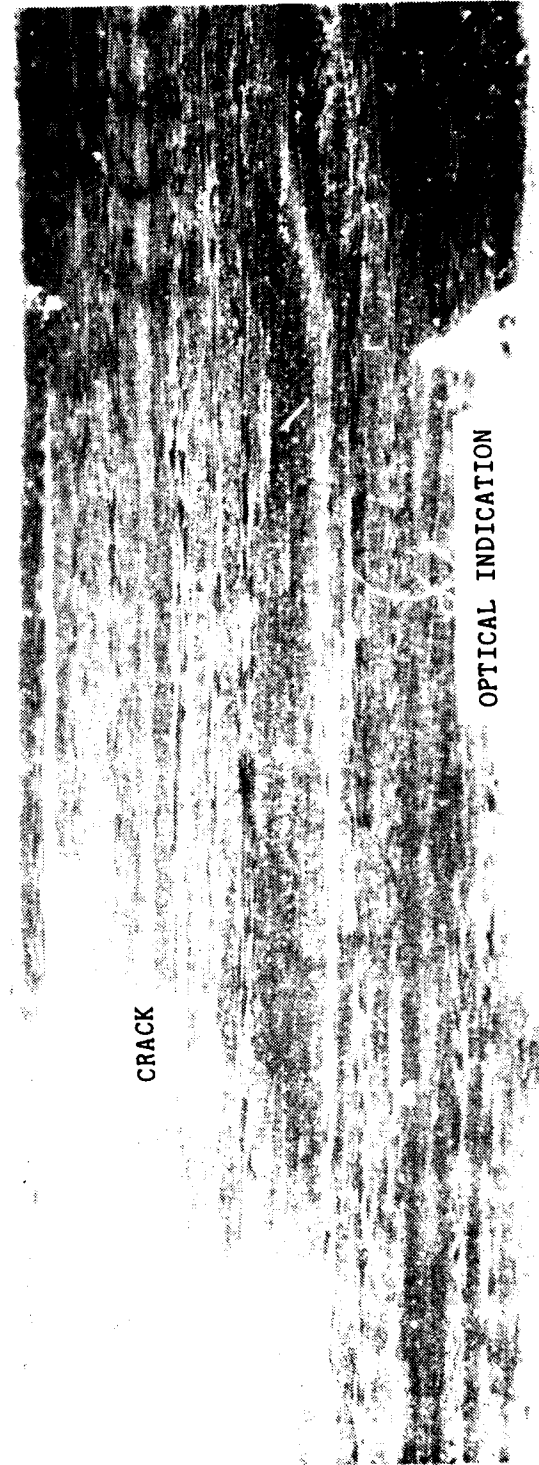
AFTER CYCLING

Figure 3.15: Replica of Left Crack Tip Rear Edge of Specimen 1YXX-3 Before and After 1100 Thermocycles.
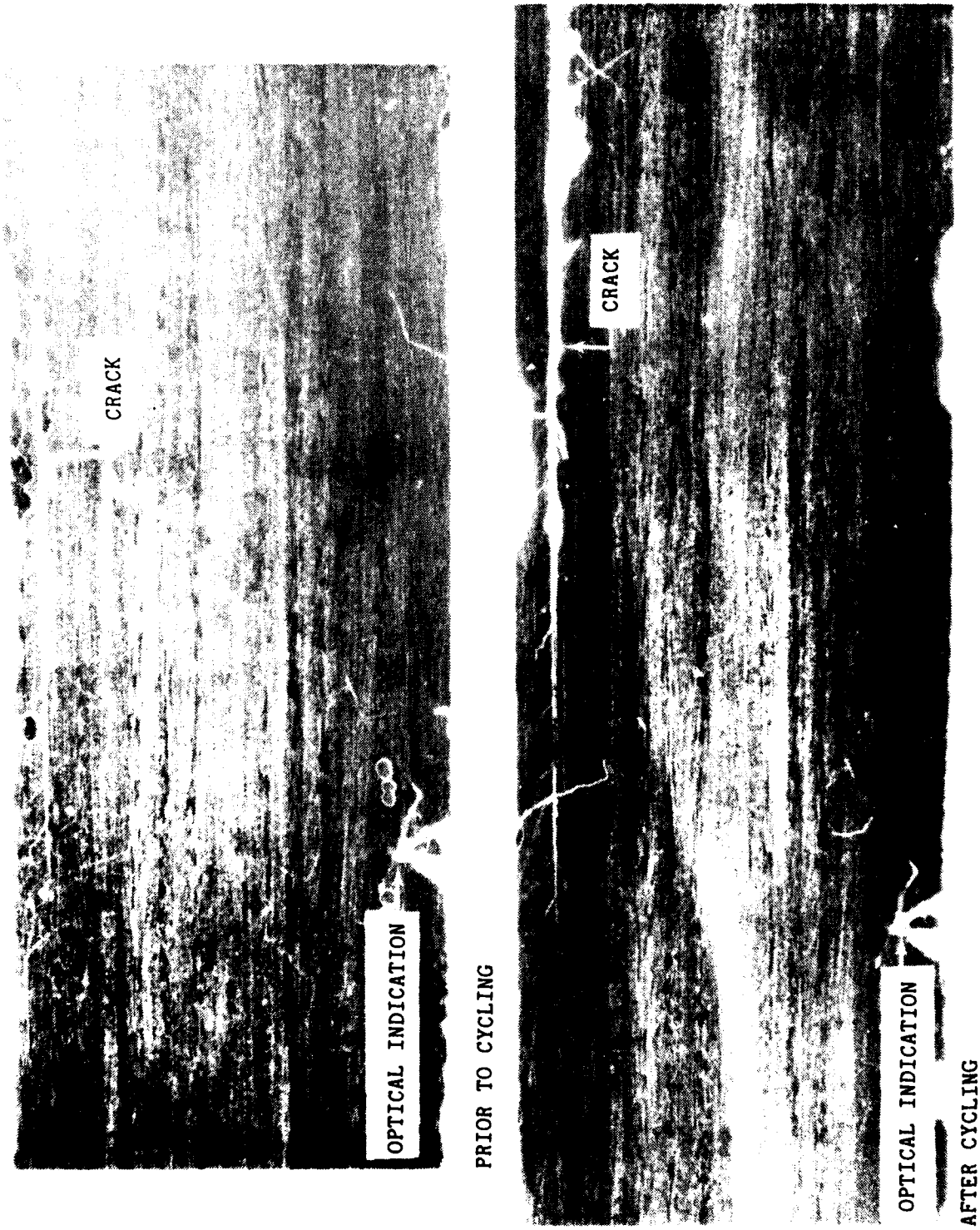
Figure 3.16: Replica of Right Crack Tip Rear Edge of Specimen 1YXX-3 Before and After 1100 Thermocycles.

CRACK

OPTICAL INDICATION

PRIOR TO CYCLING

CRACK

OPTICAL INDICATION
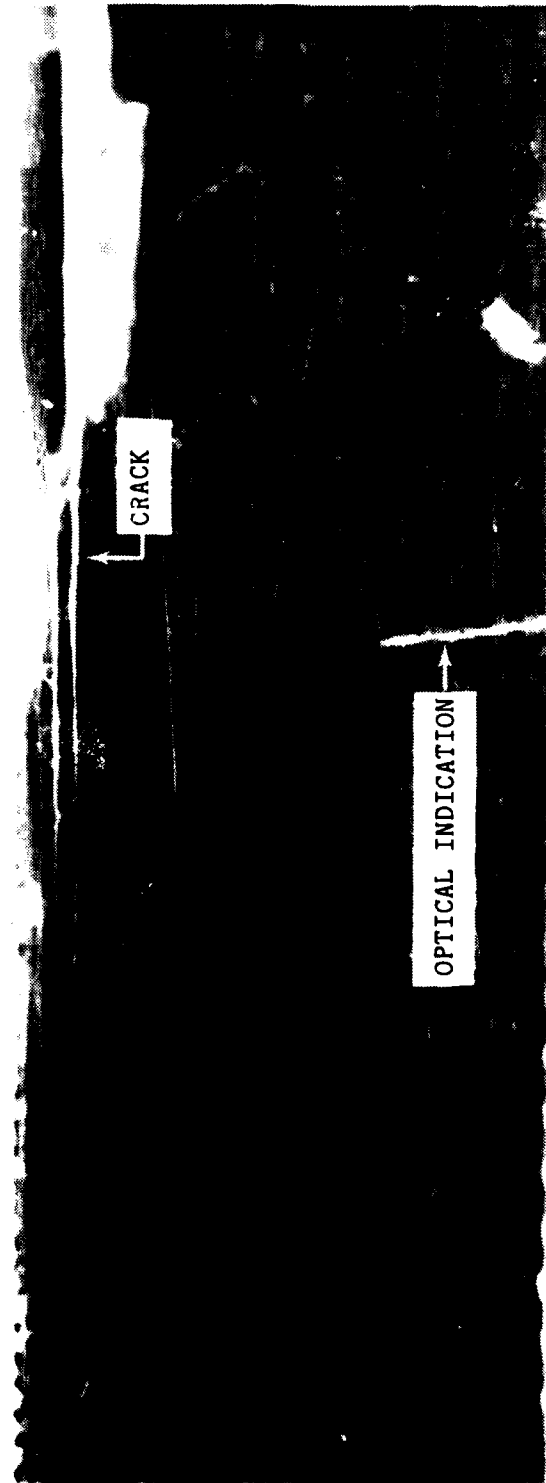
AFTER CYCLING

Figure 3.17: Replica of Left Crack Tip Front Edge of Specimen
1YXX-4 Before and After 1100 Thermocycles.

Figure 3.18: Replica of Left Crack Tip Front Edge of Specimen 1YXX-1 Before 1100 Cycles.
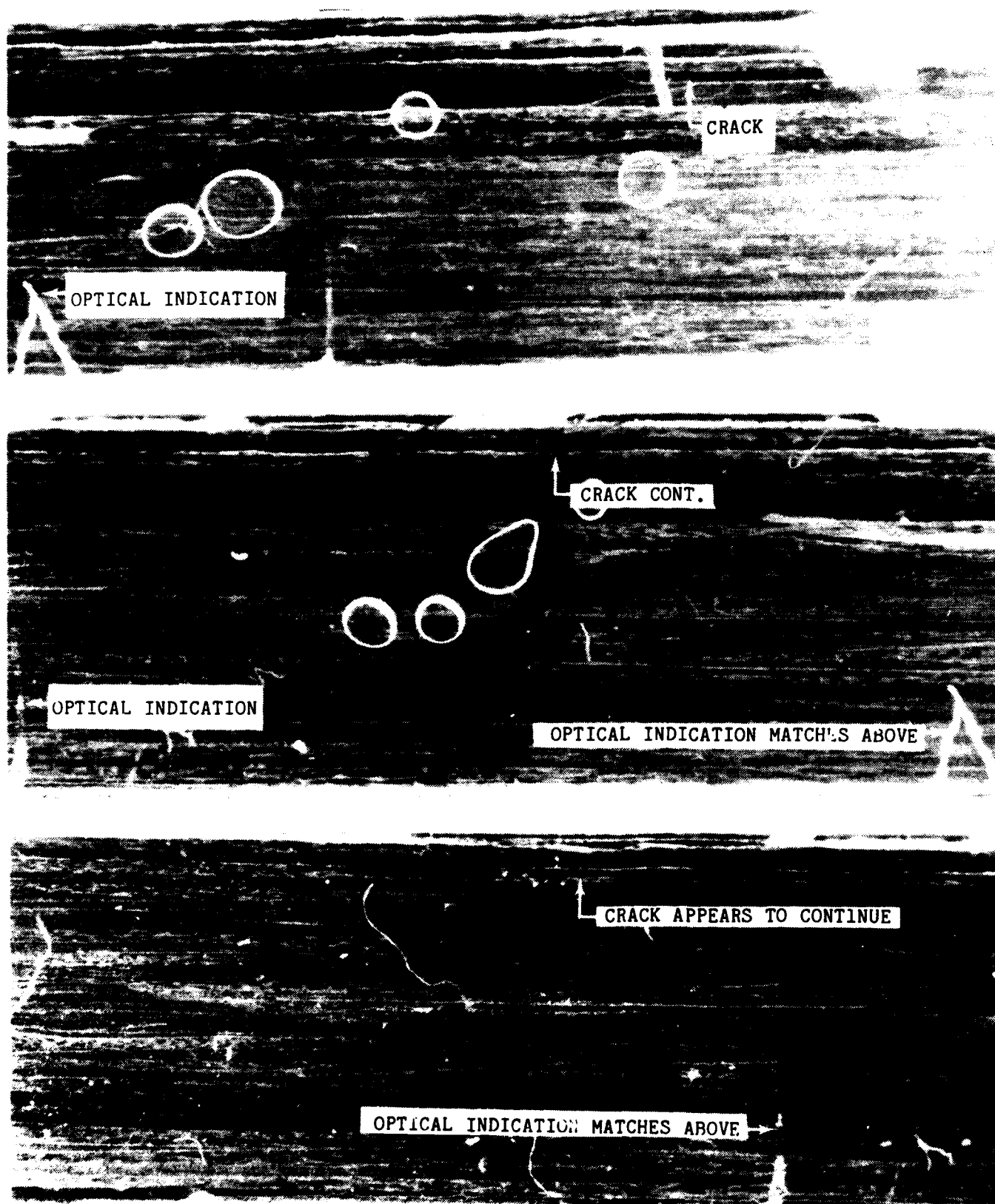
Figure 3.19: Replica of Left Crack Tip Front Edge of Specimen
1YXX-1 After 1100 Cycles.

This Page Intentionally Left Blank

SECTION 4
OBSERVATIONS AND CONCLUSIONS

Cracks do not appear to extend due to freeze-thaw cycling alone. However, this is restricted to the layup and flow type investigated in this study.

Instrumentation and test procedures are always limited in resolution by some finite value. Therefore, an absolute answer is not possible and thus acceptable limits must be defined.

When using a small sample size either the positive or negative result may be the tail fo the data distribution curve.

In the crack growth experiments the cracks were not completely found due to the need to observe crack growth at the specimen edge. However, this may not be a realistic case. Possible growth of a bound crack should be investigated.

The combined effect of mechanical load cycling and thermocycling should also be evaluated.

This Page Intentionally Left Blank

REFERENCES

1. Lauraitis, K.N., and Sandorff, P.E., "Experimental Investigation of the Interaction of Moisture, Low Temperature, and Low Level Impact on Graphite/Epoxy Composites", NADC-79102-60, Final Report, October 1980.

2. Sendeckyj, G.P., Presentation made at AFFDL Sponsored Workshop on the Nondestructive Evaluation of Composites, Wright-Patterson AFB, Ohio, October 31, 1981.

3. Interdepartmental Communication No. EL/80/74-48, from Sid Bocarsly to A.C. Jackson, "Metallographic Examination of Crown Sections After Environmental Exposure", dated March 13, 1980.

4. Lauraitis, K.N., Ryder, J.T., and Pettit, D.E., "Advanced Residual Strength Degradation Rate Modeling for Composite Structures", AFWAL-TR-79-3095, Flight Dynamics Laboratory, Air Force Wright Aeronautical Laboratories, Air Force Systems Command, Wright-Patterson Air Force Base, Ohio, May 1981.

5. Ashizawa, M., "Fast Interlaminar Fracture of a Compressively Loaded Composite Containing a Defect", Fifth DoD/NASA Conference on Fibrous Composites in Structural Design, New Orleans, Louisiana, January 1981, Douglas Paper No. 6994.

This Page Intentionally Left Blank

APPENDIX A

MATERIAL RECEIVING INSPECTION DATA AND PANEL FABRICATION DETAILS

Two 12 x 14-inch panels were fabricated for this study, identified as 1YXX1889 and 2YXX1889. Panels were fabricated from a mixture of 2 batches of AS/3501-6 graphite/epoxy material: batch code YK and batch code XO. Lockheed batch code YK material was purchased for this study while batch XO was material remaining from the previous study. The manufacturer's quality assurance data, which accompanied the shipment of the YK (Hercules Lot 1363) material, are given in Table A-1. The Lockheed QA batch acceptance data are given in Table A-2. Conformance to the specification was confirmed. The YXX panel code which designates the material batch indicates the combination. Autoclave curing followed the cycle summarized in Table A-3. Specimens were cut from the panels as shown in Figure A-1.

Analysis for fiber and resin content by weight was performed on samples of approximately one gram taken from the interior region of each panel, using techniques which (except forr the larger sample size) were in accordance with ANSI/ASTM D 792-66, Procedure A-1, for specific gravity determination, and ANSI/ASTM D 3171-73, Procedure A, for fiber content. Fiber volume fraction and void content were calculated from these data using nominal values for the specific gravity of the fiber and the resin as supplied by the manufacturer. These results, indicating fiber volume fraction between 62 and 65 percent, are summarized in Table A-4.

TABLE A-1
HERCULES INCORPORATED
QUALITY ASSURANCE CERTIFICATION

February 16, 1981

CUSTOMER: Lockheed/California

PURCHASE ORDER NO: AET1E8370G

MATERIALS: Graphite Fiber/Epoxy Material,3501-6/AS1, 12" prepreg tape.

SPECIFICATION: MMS 549, Rev. A, Type I

QUANTITY: 73.00 lbs.

LOT NO: 1779   Manufactured December 18, 1981

SPOOL NO: See Section V

RESIN LOT NO: 133   Manufactured by Hercules Inc.

FIBER LOT NO: 175-4   Manufactured by Hercules Inc.

I.   Fiber Properties

	Spec Req	Lot Average
Tensile Str.,ksi	410 minimum	482
Tensile Mod.,msi	32 - 36	34
Density,lb/in^3	0.0640-0.0660	0.0654

II.   Prepreg Physical Properties

	Spec Req	Average/Individual	Average		
Spool No.		2	1	5	9
Resin Flow,%	10 - 25		19	18	23
Volatiles,%	1.5 max.	1.2/1.3,1.2,1.2			
Tack	Table I,spec	Conforms			

III. Laminate Mechanical Properties

	Spec Req (min.ind)	Panel No. Spool		Average/Individual
			1	
0° Tensile Str.,RT,ksi*	200	12159		258/243,255,276
0° Tensile Mod.,RT,msi*	18.0	12159		21.0/20.7,20.7,21.5
0° Elongation,RT,μin/in x 10^3	10.0	12159		13.4/13.3,13.4,13.2
Short Beam Shear,RT,ksi	15.0	11763		20.0/20.5,19.9,19.7
Short Beam Shear,250°F,ksi	9.0	11763		14.3/14.1,14.4,14.4
Short Beam Shear,250°F,ksi	7.5	11763		9.9/9.9,9.8,10.1
		Spool	5	
0° Tensile Str.,RT,ksi*	200	12163		261/272,276,234
0° Tensile Mod.,RT,msi*	18.0	12163		20.6/20.8,21.6,19.6
0° Elongation,RT,μin/in x 10^3	10.0	12163		12.9/13.4,13.2,12.1
Short Beam Shear,RT,ksi	15.0	12164		20.5/21.2,20.4,20.1
Short Beam Shear,250°F,ksi	9.0	12164		13.5/12.8,13.9,13.8
Short Beam Shear,250°F,ksi (24 hour H$_2$0 boil)	7.5	12164		9.6/9.6,9.8,9.5
		Spool	9	
0° Tensile Str.,RT,ksi*	200	11878		232/212,251,234
0° Tensile Mod.,RT,msi*	18.0	11878		20.5/20.3,20.5,20.9
0° Elongation,RT,μin/in x 10^3	10.0	11878		11.5/10.5,12.5,11.4
Short Beam Shear,RT,ksi	15.0	12105		20.8/20.8,21.0,20.6
Short Beam Shear,250°F,ksi	9.0	12105		15.0/15.0,14.9,15.0
Short Beam Shear,250°F,ksi (24 hour H$_2$0 boil)	7.5	12105		10.1/9.9,10.0,10.3

* Normalized to 0.0416 Panel Thickness.   56

QUALITY ASSURANCE CERTIFICATION
Page 2
Lot No: 1779
February 16, 1981   TABLE A-1 (Continued)
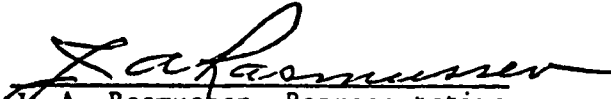
IV.   Panel Physical Properties

	Spec Req	1/12159	5/12163	9/11878
Spool No./Panel No.				
Ply Thickness, inches	0.0052 +/- 0.0003	0.0052	0.0051	0.0050

V.   Individual Spool Physical Properties

Spec Req Spool No.	Average/Individual 42 +/- 3 Resin Content, %	Average/Individual 145 - 155 Fiber Areal Wt., gm/m^2
6A	40/40,40,40	153/153,153,154
6B	44/44,43,44	153/153,153,153
1D	43/43,43,43	152/151,152,152

J. A. Rasmussen, Representative
QUALITY ASSURANCE DEPARTMENT

JAR:ln

TABLE A-2

SUMMARY OF ACCEPTANCE TESTS PERFORMED ON HERCULES AS/3501-6 MATERIAL LOT 1779 (YK)

Material Property	Specification Requirements	Measured Property		Accepted
	UNCURED PROPERTIES			
1. Areal Fiber Weight (4 req.)	146 - 162 g/m^2	153 g/m^2 156 " 159 " 159 " Ave. 157 g/m^2		X
2. Infrared Spectrophotometric Anal. (1 req.)		Filed		X
3. Volatiles (2 req.) 60 ± 5 min at 350°F	1.5% Maximum	0.73% left 0.62% left center 0.70% right 0.68% right center Ave. 0.68%		X
4. Dry resin content (4 req.)	39 - 45%	42.3% left 41.8% left center 38.4% right center 39.9% right Ave. 40.6%		X
5. Resin Flow at 350° and 85 psi (2 req.)	15 - 30%	23.0% 22.4%		X X
6. Gel Time at 350°F (2 req.)	For Information Only	16.1 Minutes		-
7. Fiber Orientation	0°	-		X
8. Resin Tack	Adhere to itself but separate after 10 min. with less than 10% damaged area.	Good tack, no damage		X

TABLE A-2 (Continued)

SUMMARY OF ACCEPTANCE TESTS PERFORMED ON HERCULES AS/3501-6 MATERIAL LOT 1779 (YK)

Material Property	Specification Requirements	Measured Property		Accepted
	CURED PROPERTIES			
1. Cured Fiber Volume, 15 Ply Panel (3 req.) for Tensile and Flex Properties	60 – 68%	63.7 61.7 63.1	Ave. 62.8	X
2. Specific Gravity, 15 Ply Panel (3 req.) for Tensile and Flex Properties	1.55 – 1.62	1.58 1.56 1.58	Ave. 1.57	X
3. Tensile Strength, Longitudinal at 75°F (3 req.) (Tensile Coupon Test)	185 ksi min.	247 240 225	Ave. 238	X
4. Elastic Modulus, Longitudinal at 75°F (3 req.) (Tensile Coupon Tests)	$18 \cdot 10^6$ psi min.	19.10^6 20.10^6 19.10^6	Ave. 19.10^6	X
5. Flexural Strength at 75°F (3 req.)	210 ksi min.	237 295 264	Ave. 265	X

TABLE A-3

AS/3501-6 CURE CYCLE

1. Apply full vacuum

2. Apply 85 ± 5 psi autoclave pressure

3. Heat to 240°F ± 10°F @ 2-4°F/min.

4. Hold at 240°F for 60 minutes

5. Raise pressure to 100 psi - Vent vacuum

6. Raise temperature to 350°F ± 10°F @ 2-5°F/min.

7. Hold at 350°F for 120 minutes

8. Cool to 200°F in not less than 30 minutes with at least 8 psi autoclave pressure

9. Post cure for 8 ± 1/2 hour at 350°F in an air circulating oven

The figure shows a specimen layout 12" wide and 14" tall with the following labels:

- 12" (top width dimension)
- 14" (left height dimension)
- Panel ID 0o
- 1¼" TRIM (top)
- ½" RESIN CONT. STRIP
- 1" TRIM (left)
- 1" TRIM (right)
- 5.25" (upper left dimension)
- 5.25" (lower left dimension)
- RELEASE STRIP (center, dashed lines)
- C̩L (right, centerline)
- 1 3/4" TRIM (bottom)
- 1.50 +0.00 -0.02
- 6 PLACES
- 1/6" CUTTING & GRINDING ALLOWANCE

- MACHINED SPECIMEN EDGES TO BE RMS 50 OR BETTER

- SPECIMEN WIDTH MUST NOT VARY BY MORE THAN 0.004 IN.

- LONG SIDES OF SPECIMEN TO BE PARRALLEL TO 0°↑ DIRECTION AND PERPENDICULAR TO C̩L

Figure A-1: Specimen Layout

TABLE A-4

FIBER AND VOID CONTENT OF PANEL MATERIAL

Panel ID		Density (gm/ml)	Resin Content by Weight (%)	Fiber Content by Volume (%)	Calculated Void Content #(%)
		1.60	29.1	63.0	0.3
1YXX 1889		1.60	29.9	62.2	-0.1
		1.60	29.4	62.6	-0.1
1YXX 1889	Avg	1.60	29.5	62.6	-
		1.61	27.5	64.9	0.1
2YXX 1889		1.61	28.5	63.8	-0.1
		1.60	27.9	64.1	0.5
2YXX 1889	Avg	1.61	28.0	64.3	-

* Fiber volume and void content calculations based on nominal values of
   density of 1.796 gm/ml for resin, as stated by manufacturer. Normal
   variations from these values frequently result in negative values for
   calculated void content.

No. of Copies

	No. of Copies
NAVAIRSYSCOM (AIR-004D)	7
(2 for retention)	
(5 for AIR-5304C)	
ONR, Washington, DC (Code 472)	1
ONR, Boston, MA.	1
NRL, Washington, Code 6120, 6306).	2
NAVSWC, Silver Spring, MD	1
WPAFB-AFML, Dayton, OH (Code LC, LN, LTF, LAE, MBC).	5
WPAFB-AFFDM, Dayton. OH (Code FDTC).	1
NAVPROPCEN, Trenton, NJ (J. Glatz).	1
NAVWPNCEN, China Lake, CA	1
NAVSEA, Washington, DC Code 6101E)	1
DTNSRDC, Bethesda, MD (Mr. Krenzke, Code 1730)	1
NASA, Langley Research Center, Hampton, VA (B. Stein).	1
ONR, Eastern Central Regional Office, Boston, MA (Ms. H. Holoch)	1
AMMRC, Watertown, MA (G. L. Hagnauer, R. Sacher)	2
Army Air Mobility R&D Laboratory, Fort Eustis, CA (J. Robinson). . .	1
Lockheed-California Co., Burbank, CA (J. W. Wooley).	1
Lockheed-Georgia Co., Marietta, GA (L. E. Meade)	1
Lockheed-Missiles & Space Co., Sunnyvale, CA (H. H. Armstrong) . . .	1
TRW, Inc., Cleveland, OH	1
DTIC	12